European Journal of Pharmaceutical Sciences xxx (2014) xxx–xxx

Contents lists available at ScienceDirect

European Journal of Pharmaceutical Sciences

journal homepage: www.elsevier.com/locate/ejps

Novel pyrazolopyrimidine derivatives targeting COXs and iNOS enzymes; design, synthesis and biological evaluation as potential anti-inflammatory agents

Q1 Ahmed H. Abdelazeem [a], Shaimaa A. Abdelatef [a], Mohammed T. El-Saadi [a], Hany A. Omar [b], Shabana I. Khan [c], Christopher R. McCurdy [d], Samir M. El-Moghazy [e,*]

[a] Department of Medicinal Chemistry, Faculty of Pharmacy, Beni-Suef University, Beni-Suef 62514, Egypt
[b] Department of Pharmacology, Faculty of Pharmacy, Beni-Suef University, Beni-Suef 62514, Egypt
[c] National Center for Natural Products Research, School of Pharmacy, The University of Mississippi, MS 38677, USA
[d] Department of Medicinal Chemistry, School of Pharmacy, The University of Mississippi, MS 38677, USA
[e] Department of Pharmaceutical Chemistry, Faculty of Pharmacy, Cairo University, Cairo 11562, Egypt

ARTICLE INFO

Article history:
Received 25 March 2014
Received in revised form 7 May 2014
Accepted 27 May 2014
Available online xxxx

Keywords:
Anti-inflammatory
Analgesic
COX
iNOS
NF-κB
Pyrazolopyrimidines

ABSTRACT

A novel set of 4-substituted-1-phenyl-pyrazolo[3,4-*d*]pyrimidine and 5-substituted-1-phenyl-pyrazolo[3,4-*d*]pyrimidin-4-one derivatives were synthesized and evaluated as potential anti-inflammatory agents. The newly prepared compounds were assessed through the examination of their *in vitro* inhibition of four targets; cyclooxygenases subtypes (COX-1 and COX-2), inducible nitric oxide synthase (iNOS) and nuclear factor kappa B (NF-κB). Compounds **8a**, **10c** and **13c** were the most potent and selective ligands against COX-2 with inhibition percentages of 79.6%, 78.7% and 78.9% at a concentration of 2 μM respectively, while compound **13c** significantly inhibited both COX subtypes. On the other hand, fourteen compounds showed high iNOS inhibitory activities with IC_{50} values in the range of 0.22–8.5 μM where the urea derivative **11** was the most active compound with IC_{50} value of 0.22 μM. Most of the tested compounds were found to be devoid of inhibitory activity against NF-kB. Moreover, almost all compounds were not cytotoxic, (up to 25 μg/ml), against a panel of normal and cancer cell lines. The *in silico* docking results were in agreement with the *in vitro* inhibitory activities against COXs and iNOS enzymes. The results of *in vivo* anti-inflammatory and antinociceptive studies were consistent with that of *in vitro* studies which confirmed that compounds **8a**, **10c** and **13c** have significant anti-inflammatory and analgesic activities comparable to that of the control, ketorolac. Taken together, dual inhibition of COXs and iNOS with novel pyrazolopyrimidine derivatives is a valid strategy for the development of anti-inflammatory/analgesic agents with the probability of fewer side effects.

1. Introduction

Over the past several decades, the quest to discover novel remedies for inflammation has resulted in new chemical entities with more improved therapeutic efficacy and lower toxicity than the existing anti-inflammatory drugs. It is well-documented that the inflammation process involves a sequential activation of signaling molecules, proinflammatory mediators, such as prostaglandins (PGs) and nitric oxide (NO) which are generated by cyclooxygenases (COXs) and nitric oxide synthase (iNOS) respectively (Ialenti et al., 1992; Ianaro et al., 1994; Salvemini et al., 1995; Seibert et al., 1994). PGE_2 is an important prostaglandin, which plays a crucial role in regulation of vascular permeability, platelet aggregation, and thrombus formation through the progression of inflammation.

Currently, it is well documented that there are, at least two designated COX isoforms; COX-1 and COX-2 (Dannhardt and Kiefer, 2001; Gund and Shen, 1977). COX-1 is the constitutive isoform which is widely expressed in most tissues and it is responsible for the synthesis of cytoprotective PGs in GIT, maintenance of normal renal function and the biosynthesis of pro-aggregatory TXA2 in blood platelets (Almansa et al., 2003; Yoshimura et al., 2011). The inducible COX-2 is the second isoform which is prominent at sites of inflammation and it is rapidly induced in response to mitogenic and proinflammatory stimuli. COX-2 significantly

* Corresponding author. Address: Department of Pharmaceutical Chemistry, Faculty of Pharmacy, Cairo University, Kasr-El-Eini Street, Cairo 11562, Egypt. Tel.: +20 002 01223662720.
E-mail address: drsamirelmoghazy@yahoo.com (S.M. El-Moghazy).

http://dx.doi.org/10.1016/j.ejps.2014.05.025
0928-0987/© 2014 Published by Elsevier B.V.

contributes in the production of inflammatory PGs (Peri et al., 1995). Traditional non-steroidal anti-inflammatory drugs (NSAIDs) which inhibit both COX subtypes are still the most commonly used medications for inflammation and pain (Salgin-Goksen et al., 2007). However, it is well known that NSAIDs have several serious side effects such as gastric ulceration, renal injury and cardiotoxicity (Allison et al., 1992; Wolfe et al., 1999). To limit the risk of GI damage induced by NSAIDs, highly selective COX-2 inhibitors (coxibs) have been developed where they exhibited equivalent anti-inflammatory/analgesic activities to those of non-selective COX inhibitors but with least GI toxicity (Micklewright et al., 2003).

Furthermore, the inducible transcription factor (NF-kB) regulates the expression of several genes such as iNOS, COX-2, and TNF-α that are involved in inflammatory responses at the transcriptional level (Ghosh and Karin, 2002). Meanwhile, iNOS is responsible for overproduction of the endogenous free radical nitric oxide (NO) in the inflammation site. This free radical is an important mediator in the process of vasodilation, nonspecific host defense, and acute or chronic inflammation causing tissue injuries (Cirino et al., 2006; Clancy et al., 1998; MacMicking et al., 1997). Therefore, it has been proposed that a combined inhibition of COX-2 and iNOS would be a useful and proper strategy for the treatment of inflammatory diseases by suppression of the overproduction of PGE_2 and NO respectively (Lim et al., 2009; Ma et al., 2011).

The pyrazolopyrimidine fused heterocyclic system is a frequently found scaffold in a wide variety of bioactive molecules including antivirals (Chern et al., 2004; El-Bendary and Badria, 2000), antimicrobials (Abunada et al., 2008; Bakavoli et al., 2010; Bondock et al., 2008), anticancer (Celano et al., 2008; Spreafico et al., 2008), antileukemic (Cottam et al., 1984), CNS agents Q2 (Chen, 2000), tuberculostatic (Trivedi et al., 2010, 2012), antileishmanials (Looker et al., 1986), anticardiovascular diseases (Guccionea et al., 1996; Xia et al., 1997) and anti-inflammatory agents (Rathod et al., 2005; Yewale et al., 2012). Recently, Yewale et al. synthesized and evaluated a novel series of 3-substituted-1-aryl-5-phenyl-6-anilinopyrazolo[3,4-*d*]pyrimidin-4-ones as potential anti-inflammatory agents. Compound **1** exhibited superior anti-inflammatory activity in comparison with diclofenac sodium and comparable activity with celecoxib at a dose of 25 mg/kg, Fig. 1 (Yewale et al., 2012). Moreover, the pyrazolopyrimidine derivative **2** was reported to inhibit selectively and potently COX-2 activity in human monocytes (IC_{50} = 0.9 nM for COX-2 vs. IC_{50} = 59.6 nM for COX-1) with anti-angiogenic activity as well.(-Devesa et al., 2004; Quintela et al., 2003) Raffa et al. prepared and evaluated a set of 5-benzamido-1*H*-pyrazolo[3,4-*d*]pyrimidin-4-ones as anti-inflammatory agents. Compound **3** revealed a better inhibitory profile against COX-2 than that of reference compounds N-[2-(cyclohexyloxy)-4-nitrophenyl] methanesulphonamide (**NS398**) and indomethacin (Raffa et al., 2009). Furthermore, the piperazine ring system is a common core template in various pharmacologically active compounds toward several receptors, especially G-coupled receptors, such as 5-HT and sigma receptor subtypes (Mesangeau et al., 2008; Seminerio et al., 2012). Also, it was found that some compounds containing piperazine core such as compound **4** display good anti-inflammatory and analgesic activity, Fig. 1 (Gökhan et al., 1996; Viaud et al., 1995).

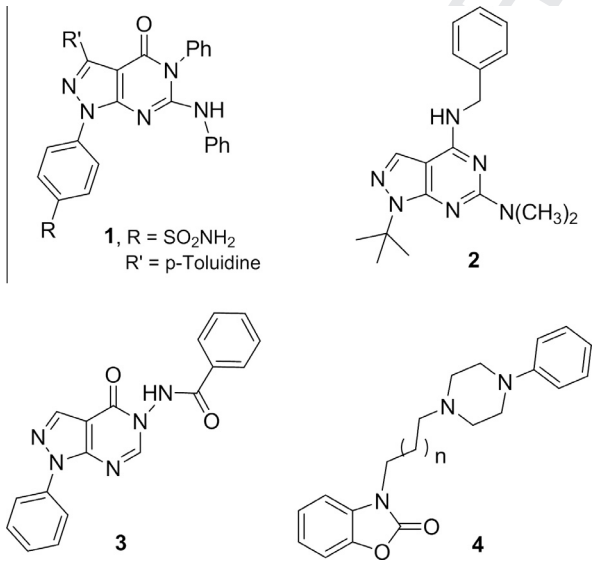

Fig. 1. Chemical structures of some reported pyrazolo[3,4-*d*]pyrimidine and piperazine derivatives with anti-inflammatory potential (Devesa et al., 2004; Gökhan et al., 1996; Quintela et al., 2003; Raffa et al., 2009; Viaud et al., 1995; Yewale et al., 2012).

Based on the aforementioned studies and the substantial need for superior anti-inflammatory compounds devoid of the classical NSAIDs liabilities, we have undertaken the synthesis of novel pyrazolopyrimidine derivatives as COXs and iNOS dual inhibitors with the hope of realizing compounds with improved anti-inflammatory/analgesic activity and diminished side effects. Our strategy to accomplish these goals was to tether the pyrazolopyrimidine system to various piperazine derivatives or sulfonamides at positions 4 and 5 utilizing a fragment-based drug design approach.

2. Results and discussion

2.1. Chemistry

All the target compounds were prepared according to the synthetic pathways outlined in Schemes 1–3. The synthesis of the new pyrazolopyrimidine derivatives proceeded through the general intermediate, 5-amino-1-phenyl-4-cyanopyrazole (**5**) which was obtained through the reaction of phenylhydrazine with commercially available ethoxymethylenemalononitrile in alcohol with a good yield (Cheng and Robins, 1956). The preparation of 1-phenyl-pyrazolo[3,4-*d*]pyrimidin-4-one (**6**) was accomplished by heating the starting material **5** with formic acid which, in turn was N-alkylated with excess dibromoethane in the presence of sodium hydride as a base to give intermediate **7**. The coupling reaction of the bromo intermediate **7** with various primary and secondary amines upon heating in DMF and potassium carbonate afforded the final compounds **8a**–**f**. The chloro derivative **8g** was formed via the treatment of compound **8f** with excess thionyl chloride in chloroform, as shown in Scheme 1.

On the other hand, heating of compound **5** with formamide in ethanol gave the corresponding 1-phenyl-pyrazolo[3,4-*d*]pyrimidin-4-amine (**9**) which was subsequently treated with various aldehydes through reductive amination using sodium triacetoxyborohydride in dichloroethane to afford the target compounds **10a**–**c**. In addition, condensation of compound **9** with phenylisocyanate in DCM provided the desired urea derivative **11**, in a high yield. The treatment of 1-phenyl-pyrazolo[3,4-*d*]pyrimidin-4-one (**6**) with phosphorus oxychloride in dimethyl formamide yielded 4-chloro-1-phenyl-pyrazolo[3,4-*d*]pyrimidine **12** which then was utilized for the synthesis of pyrazolopyrimidine derivatives **13a-m** by nucleophilic displacement of the chlorine atom with various piperazine derivatives and other amines, as shown in Scheme 2. It should be mentioned that **13c** was reported earlier as a Trp-p8 modulator and it had been synthesized by a different procedure (Natarajan et al., 2005). Compound **13l** was selected for further structural modification to study the effect of incorporating new

Please cite this article in press as: Abdelazeem, A.H., et al. Novel pyrazolopyrimidine derivatives targeting COXs and iNOS enzymes; design, synthesis and biological evaluation as potential anti-inflammatory agents. Eur. J. Pharm. Sci. (2014), http://dx.doi.org/10.1016/j.ejps.2014.05.025

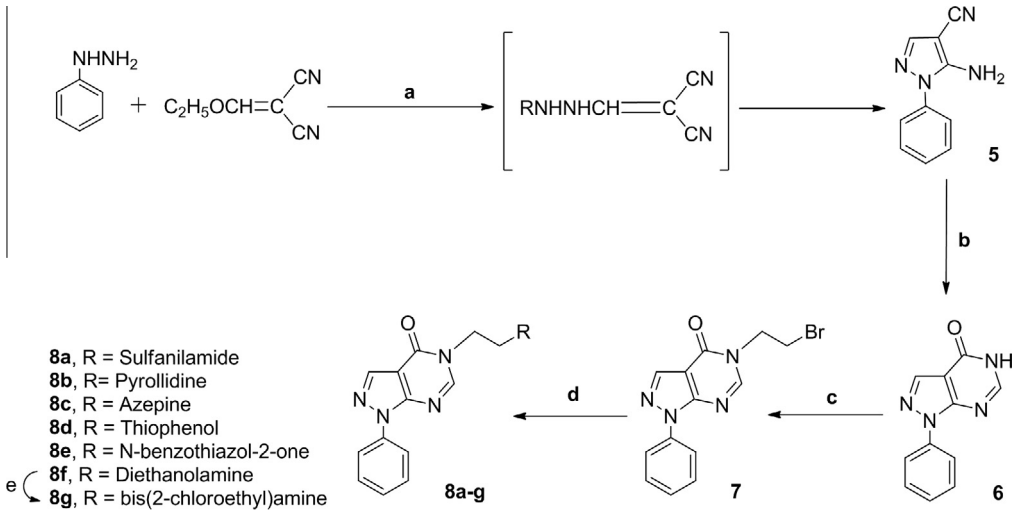

Scheme 1. [a]Reagents and reaction conditions: (a) ethanol, rt, overnight; (b) HCOOH, reflux, 6 h; (c) dibromoethane, NaH, DMF, 0 °C - rt; (d) appropriate amine, K_2CO_3, DMF, 60 °C; (e) $SOCl_2$, $CHCl_3$, reflux, 2 h.

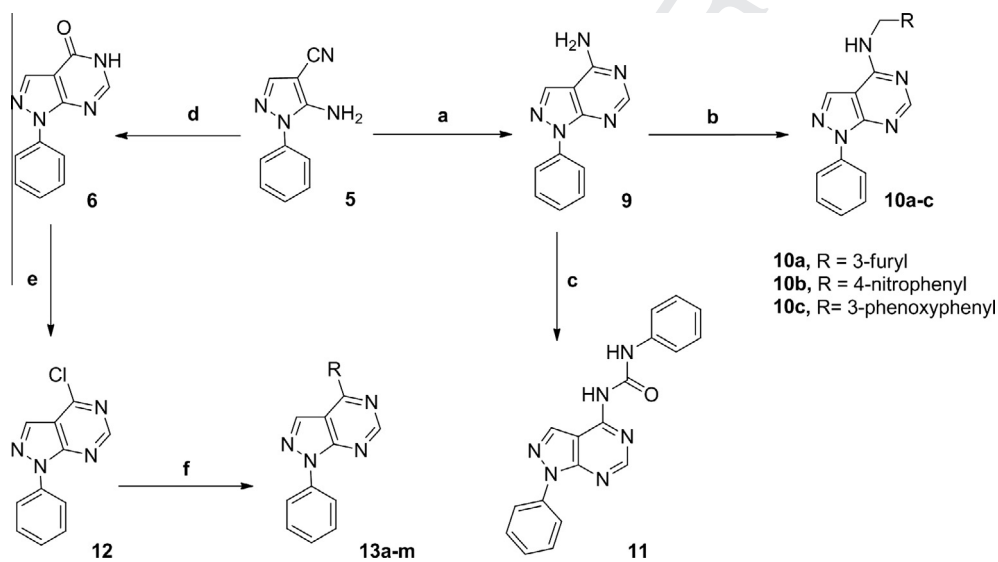

Scheme 2. [a]Reagents and reaction conditions: (a) formamide, reflux, 4 h; (b) appropriate aldehyde, sodium triacetoxyborohydride, DCE, rt, overnight; (c) phenylisocyanate, DCM, rt, overnight; (d) HCOOH, reflux, 6 h; (e) $POCl_5$, DMF, reflux, 2 h; (f) appropriate amine, Ethanol, reflux, 2 h.

groups such as *gem*-difluoro or increasing its size on the activity. The introduction of the *gem*-difluoro substituent in 1-(1-phenylpyrazolo[3,4-*d*]pyrimidin-4-yl) piperidin-4-one **13l** was achieved by treatment of **13l** with deoxofluor in DCM at 0 °C to afford compound **14** (Robichaud et al., 2008). Meanwhile, the condensation reaction of **13l** with *o*-hydroxyacetophenone proceeded in methanol and was mediated by pyrrolidine afforded the spiro derivative **15**. Subsequent reduction of **13l** with sodium borohydride in methanol and reductive amination (Abdel-Magid et al., 1996) with sulfanilamide using sodium triacetoxyborohydride in dichloroethane gave the corresponding target compounds **17** and **16** respectively depicted in Scheme 3.

2.2. Pharmacology

The newly synthesized pyrazolopyrimidine derivatives were evaluated through *in vitro* and *in vivo* assays for their anti-inflammatory and analgesic potentials. All compounds were initially underwent *in vitro* screening in cellular assays to examine their inhibitory activities on three targets; COXs, iNOS and NF-κB. The results of iNOS and NF-κB inhibitory assays were expressed in terms of IC_{50} values (the concentration that caused a 50% inhibition) while the inhibition of COX-1 and COX-2 was expressed in terms of% inhibition at 2 μM as displayed in Table 1. In addition, the cytotoxicity of all the compounds was determined against a panel of normal and cancerous mammalian cell lines. Based on the *in vitro* assays results, the most active eight compounds were selected to be tested for their *in vivo* efficacy. Three *in vivo* measures were utilized; the carrageenan-induced paw hyperalgesia assay was used for testing the anti-hyperalgesia, the carrageenan-induced paw edema assay was used for assessment of the anti-inflammatory activity and finally, acetic acid-induced writhing assay was used for evaluating the anti-nociception potential.

2.2.1. Inhibition of COX subtypes activity

Thirteen representative compounds were selected to be tested for their ability to inhibit COX-1 and COX-2 enzyme activity. The

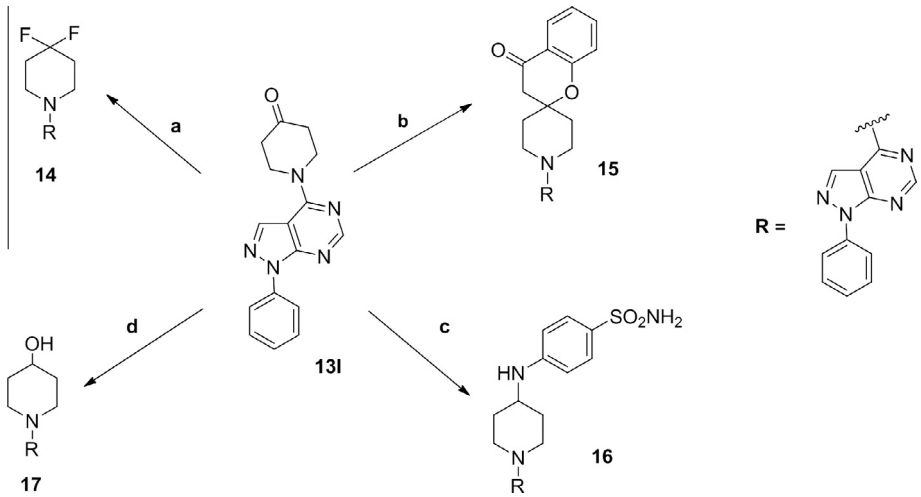

Scheme 3. [a]Reagents and reaction conditions: (a) deoxofluor, DCM, 0 - rt °C, overnight; (b) 2-hydroxyacetophenone, pyrrolidine, reflux, 6 h; (c) sulfanilamide, sodium triacetoxyborohydride, DCE, rt, overnight; (d) $NaBH_4$, MeOH, 0 °C, 2 h.

results revealed that compounds **8a**, **10c** and **13c** were the most potent and the most selective ligands against COX-2 with inhibition percentages of 79.6%, 78.7% and 78.9%, at a concentration of 2 μM respectively. On the other hand, compounds **8e**, **13e**, **13m**, **15** and **16** showed moderate activity against COX-2 with inhibition percentages of 42.9%, 24.9%, 38.9%, 43% and 33%, respectively. On the contrary, compounds **8d** and **13a** exhibited a good selectivity against COX-1 with moderate inhibition percentages of 28.7% and 22.4%, respectively. Moreover, compound **13b** was non-selective ligand that could inhibit both COX subtypes with moderate inhibition percentages of 43.1% for COX-1 and 37.5% for COX-2 respectively. It could be suggested that the sulfonamide moiety in compounds, **8a**, **13n** and **16** may largely contribute to their COX-2 selectivity. However, compounds **8e**, **10c**, **13c**, **15** and **13e** have COX-2 selectivity and they do not incorporate a sulfamoyl ($-SO_2NH_2$) moiety in their structures. This finding could affirm that the importance of sulfonamide as a structural basis for COX-2 selectivity is still controversial. Interestingly, the 4-substituted pyrazolopyrimidines (Scaffold **B**) were more active than the 5-substituted derivatives (Scaffold **A**). The structure activity relationship for the whole series needs further studies to be explained in details. However, *in silico* docking studies confirmed the main structural features required for activity and selectivity against both COX subtypes.

2.2.2. Inhibition of iNOS activity

The iNOS inhibitory assay was performed in LPS-induced mouse macrophages (RAW264.7) where the concentration of NO was determined by measuring the level of nitrite in the cell culture supernatant using *Griess* reagent. Parthenolide was used as positive control. It was found that most of the newly synthesized pyrazolopyrimidines exerted good to moderate inhibitory activities with IC_{50} values between 0.22 and 8.5 μM. In general, it was noticed that the substitution at position 5 was more favorable for the iNOS activity than the substitution at position 4 of the pyrazolopyrimidine scaffold. Compounds **8a**–**8g**, except compounds **8b** and **8f**, showed remarkable activity with IC_{50} values between 0.24 and 0.71 μM. It was apparent that replacement of the azepine moiety with the smaller pyrrolidine, abolished the activity in compound **8b**. On the other hand, the replacement of the electron withdrawing group (chloride) in compound **8g** with a hydroxyl group in compound **8f** abolished the activity as well. Regarding the substitution at position 4 of the pyrazolopyrimidine nucleus, the urea derivative **11** was the most active derivative with IC_{50} value of 0.22 μM. The introduction of a bulky phenoxybenzyl, as in compound **10c**, was well tolerated inside the extended iNOS binding site and it exerted high activity with IC_{50} value of 0.3 μM. In contrast, the less bulky compound **10a** and the nitro derivative **10b** were inactive. For piperazine derivatives, it was observed that the phenylpiperazine derivatives bearing an electron withdrawing group were more active than those containing electron donating moieties. Compounds **13c**, **13e**, **13h** and **13j** were active ligands with IC_{50} values of 0.4, 0.97, 2.8 and 2.1 μM respectively. On the other hand, compounds **13b**, **13d**, **13f**, **13i** and **13k** were less active or devoid of any iNOS inhibitory activity. In addition, the piperidin-4-one derivative **13l** was more active than the piperidin-4-ol derivative **17** with intermediate IC_{50} values. Despite of the bulkiness of the spiro derivative **15**, it showed no activity which confirmed the size of the ligand is crucial for activity. Finally, the *gem*-difluoro derivative **14** possessed moderate activity with IC_{50} value of 3.8 μM while sulfonamide compounds **13m** and **16** were inactive.

2.2.3. Inhibition of NF-κB transcriptional activity

All compounds were devoid of any activity against NF-kB except compounds **8e** and **13d** which exhibited moderate inhibition with IC_{50} values of 5.3 and 2.8 μM respectively.

2.2.4. Cytotoxicity

All novel pyrazolopyrimidine derivatives were evaluated for cytotoxicity against a panel of four human solid tumor cell lines (SK-MEL: malignant melanoma; KB: oral epidermal carcinoma; BT-549: breast ductal carcinoma, and SK-OV-3: ovary carcinoma) as well as and two normal kidney cell lines (Vero: monkey kidney fibroblasts and LLC-PK_1: pig kidney epithelial cells). In addition, all compounds were tested against Mouse leukemic monocyte macrophage cells (RAW 264.7) to determine whether their iNOS inhibitory activity was related to a decrease in cell viability due to the toxicity of tested compounds. Most of the compounds were not cytotoxic up to a concentration of 25 μg/mL and do not seem to have any significant anti-cell proliferative activity toward cancer cells or any observable cytotoxic effect toward the normal cells except compound **13a** which showed cytotoxicity in LLC-PK_1 cells at high concentrations (IC_{50} values 42.35 and 37.83 μM, respectively). The results are shown in Table 2.

2.2.5. Carrageenan-induced rat paw edema assay

The assessment of anti-inflammatory activity of the selected eight compounds was performed using carrageenan-induced rat

Table 1
Inhibition of COX-1, COX-2, iNOS and NF-kB by the newly synthesized pyrazolopyrimidine derivatives.

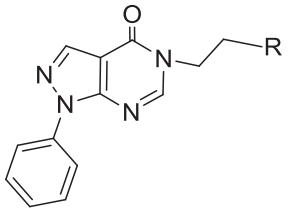
(A)

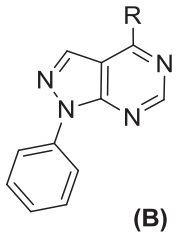
(B)

Compound	Scaffold	R	% Inhibition at 2 μM		IC_{50} (μM)	
			COX-1	COX-2	iNOS	NF-kB
7	**A**	Br	ND	ND	0.78	NA
8a	**A**	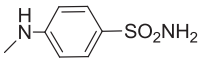	NA	79.60	0.34	NA
8b	**A**		ND	ND	NA	NA
8c	**A**		ND	ND	0.27	NA
8d	**A**	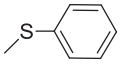	28.70	NA	0.71	NA
8e	**A**	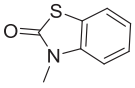	NA	42.90	0.38	5.3
8g	**A**	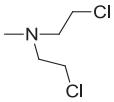	ND	ND	0.24	NA
10a	**B**	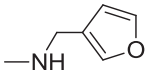	ND	ND	ND	ND
10b	**B**	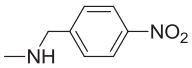	ND	ND	5.2	NA
10c	**B**	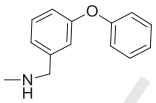	NA	78.70	0.30	NA
11	**B**	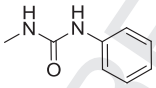	NA	NA	0.22	NA
13a	**B**	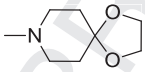	22.40	2.30	NA	NA
13b	**B**	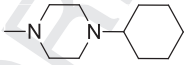	43.10	37.50	4.4	NA
13c	**B**	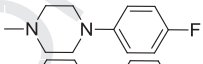	NA	78.90	0.40	NA
13d	**B**	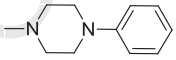	ND	ND	NA	2.8
13e	**B**	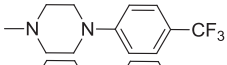	NA	24.90	0.97	NA
13f	**B**	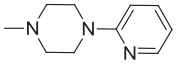	ND	ND	NA	NA
13g	**B**	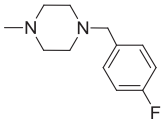	ND	ND	NA	NA
13h	**B**	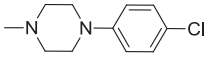	ND	ND	2.8	NA
13i	**B**	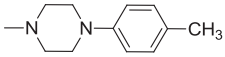	ND	ND	NA	NA
13j	**B**	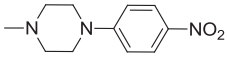	NA	NA	2.1	NA

(*continued on next page*)

Please cite this article in press as: Abdelazeem, A.H., et al. Novel pyrazolopyrimidine derivatives targeting COXs and iNOS enzymes; design, synthesis and biological evaluation as potential anti-inflammatory agents. Eur. J. Pharm. Sci. (2014), http://dx.doi.org/10.1016/j.ejps.2014.05.025

Table 1 (*continued*)

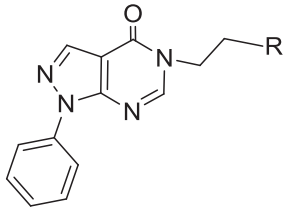
(A)

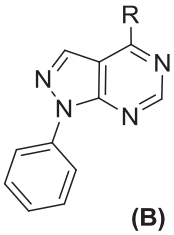
(B)

Compound	Scaffold	R	% Inhibition at 2 μM		IC_{50} (μM)	
			COX-1	COX-2	iNOS	NF-kB
13k	**B**	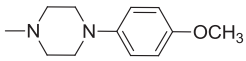	ND	ND	NA	NA
13l	**B**	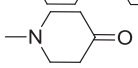	NA	NA	6.3	NA
13m	**B**	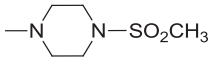	NA	38.9	NA	NA
14	**B**	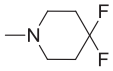	ND	ND	3.8	NA
15	**B**	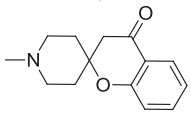	14.90	43.00	NA	NA
16	**B**	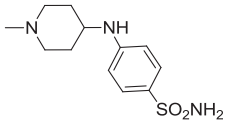	NA	33.00	NA	NA
17	**B**	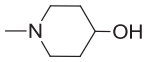	ND	ND	8.5	NA
Indomethacin	–	–	92.10	24.60	–	–
Parthenolide	–	–	–	–	0.015	0.02

Inhibition of COX-1 and COX-2 is represented in terms of % inhibition at 2 μM. Inhibition of iNOS and NF-kB is represented in terms of IC_{50} values obtained from dose response curves. **NA** = No activity was observed up to 50 μM. **ND** = Not determined. **Positive controls**: indomethacin for COX inhibition and Parthenolide for iNOS and NF-κB inhibition.

Table 2
In vitro cytotoxicity of newly synthesized pyrazolopyrimidine derivatives.

Compound	IC_{50} values μM						
	SK-MEL	KB	BT-549	SK-OV-3	VERO	LLC-PK11	RAW 264.7
7	NC	NC	NC	NC	NC	NC	NC
8a-g	NC	NC	NC	NC	NC	NC	NC
10a-c	NC	NC	NC	NC	NC	NC	NC
13a	NC	NC	NC	NC	NC	37.83	NC
13b-m	NC	NC	NC	NC	NC	NC	NC
14	NC	NC	NC	NC	NC	NC	NC
15	NC	NC	NC	NC	NC	NC	NC
17	NC	NC	NC	NC	NC	NC	NC
Doxorubicin	–	2.75	2.00	2.57	12.9	2.20	ND

Cytotoxicity was determined in a panel of cell lines which included human solid tumor cell lines [SK-MEL (Melanoma), KB (epidermal carcinoma), BT-549 (breast carcinoma) and SK-OV-3 (ovarian carcinoma)], normal kidney cell lines [Vero (Monkey kidney fibroblast) and LLC-PK_1 (Pig kidney epithelial cells)] and Mouse leukemic monocyte macrophage cells (RAW 264.7).
Doxorubicin for was used as **positive control** in cytotoxicity assay.
NC = No cytotoxicity.

paw edema model using ketorolac as a reference anti-inflammatory drug. Mean changes in paw edema thickness of animals pretreated with the test compounds after 1, 3 and 6 h from induction of inflammation is shown in Fig. 2. The results were in accordance with the *in vitro* results of the compounds in both COX and iNOS assays where compounds **8a**, **10c** and **13c** showed the most potent anti-inflammatory activities compared to ketorolac. However, compounds **13b** and **13m** displayed moderate anti-inflammatory activities and this could be explained by their weak to moderate activities on both COXs and iNOS targets. On the contrary, the least potent compounds were **8c** and **10b** which showed no activity *in vitro* against COX subtypes although they showed considerable inhibition of iNOS.

2.2.6. Carrageenan-induced thermal hyperalgesia assay

To evaluate the analgesic activity of eight compounds from the newly synthesized pyrazolopyrimidine derivatives, carrageenan-induced thermal hyperalgesia model was used. Ketorolac was used as a reference analgesic drug. Fig. 3 shows the withdrawal latency of the test compounds compared to vehicle-treated animals at the

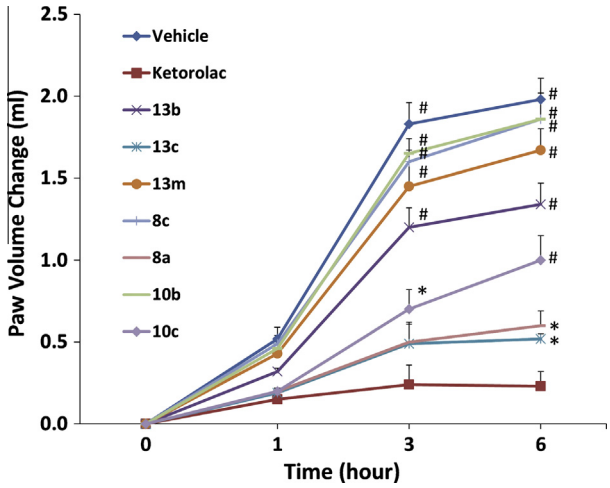

Fig. 2. Results of carrageenan-induced rat paw edema assay. Data are mean ± SD ($N = 6–8$). $^{*}P < 0.05$, $^{\#}P < 0.01$ represents significant change in paw volume changes compared to vehicle-treated group.

indicated time points. All the tested compounds, except **8c** and **10b**, showed variable analgesic activities. Compounds **8a**, **10c** and **13c** showed potent analgesic activities compared to ketorolac while compounds **13b** and **13m** displayed moderate analgesic activities. It was noteworthy that these results were consistent with the *in vitro* inhibitory values of the same compounds on both COX and iNOS where compounds **8a**, **10c** and **13c** showed the highest COX-2 inhibition percentages of 79.60, 78.70 and 78.90% respectively. Also, these three compounds have good iNOS inhibitory IC_{50} values of 0.34, 0.30, 0.40 μM respectively.

2.2.7. Acetic acid-induced writhing test

Test compounds were further investigated for their analgesic activity using the acetic acid-induced writhing test in mice. Ketorolac was used as a reference standard analgesic drug. Four compounds (**13b**, **13c**, **8a**, **10c**) exhibited relatively good analgesic activity compared to the used standard analgesic, ketorolac. The most active compound was **13c** which also has a good activity against both COX-2 and iNOS as mentioned previously. The effects of the drug probes on the acetic acid abdominal writhing assay are summarized in Fig. 4.

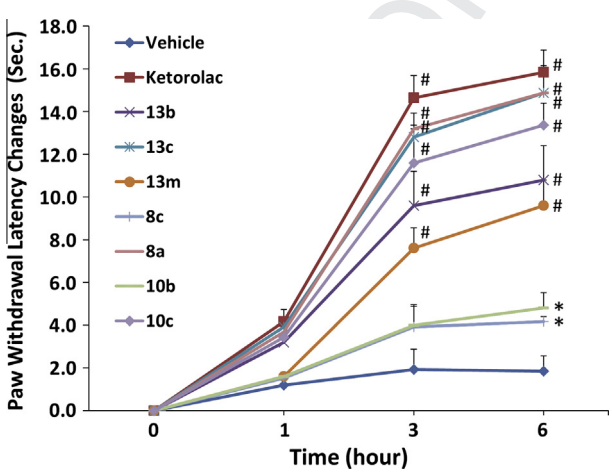

Fig. 3. Results of carrageenan-induced thermal hyperalgesia assay. Data are mean ± SD ($N = 6–8$). $*P < 0.05$, $^{\#}P < 0.01$ represents significant change in paw withdrawal latency changes compared to vehicle-treated group.

2.3. Docking studies

To shed light into the required structural features for the activity and the proper binding mode of the newly synthesized pyrazolopyrimidine ligands, some of these compounds were docked into the active sites of both COX subtypes and iNOS by using LIGANDFIT embedded in Discovery Studio software (Accelrys Software Inc., 2007). The protein crystal structures of COX-1, COX-2 and iNOS complexed with their cocrystallized inhibitors (PDB codes: **1PGF**, **1CX2** and **3E65**, respectively) were selected for this study. It was reported that the substitution of **Ile523** in COX-1 with the less bulky **Val523** in COX-2 creates an additional polar side pocket and increases the volume of the COX-2 active site that makes it accommodate more bulky structures (Kurumbail et al., 1996). The presence of such side pocket allows additional interactions with amino acids such as **Arg513**, replaced by a **His513** in COX-1. The structure of traditional COX-2 inhibitors exploits binding with **Arg513** in the COX-2 side-pocket, often via sulfone or sulfonamide groups, to accomplish their selectivity.

In this regard, we examined the docking results of two of the most COX-2 active newly synthesized pyrazolopyrimidines, **8a** and **10c**, into COX-2 active sites. It was clear that the binding mode and interactions of our compounds were similar with the cocrystallized bromocelecoxib, SC-558 ligand. Clearly from Fig. 5(**A**), positioning the sulfonamide moiety of **8a** within the side pocket of COX-2 and forming H-bond with NH of Arg513 residue was similar to fitting of same moiety of SC-558 into the same side pocket in addition to forming two H-bonds with NHs of Arg513 and His90 residues, Fig. 5(C). Interestingly, the side pocket of COX-2 could accommodate the phenoxy ring of **10c** which showed a similar binding pattern and orientation within the entire COX-2 active site. In addition, **10c** phenoxy formed an H-bonding interaction with Arg513 residue which is important for COX-2 selectivity, Fig. 5(**B**). Furthermore, positioning the phenyl ring attached to the pyrazolopyrimidine nucleus in both **8a** and **10c** within the hydrophobic pocket of the side chains of Tyr348 and Trp387, correlates well with the position of the bromophenyl fragment of SC-558 into the same pocket via p-stacking interactions, Fig. 5. On the other hand, docking of **8d** and **13a** revealed that both compounds were forced to adopt another binding position within the long COX-1 binding pocket due to presence of Ile523 which prevented the formation of the side pocket and pushed the compounds to the bottom of the active site. Fig. 6 shows the similar analogy between the aromatic hydrophobic stacking of the phenyl ring in **8d** and **13a** with the aromatic residues in Trp387 and Tyr385 and the iodophenyl in the IMM cocrystallized ligand with the same residues. We can also notice the H-bonding interaction

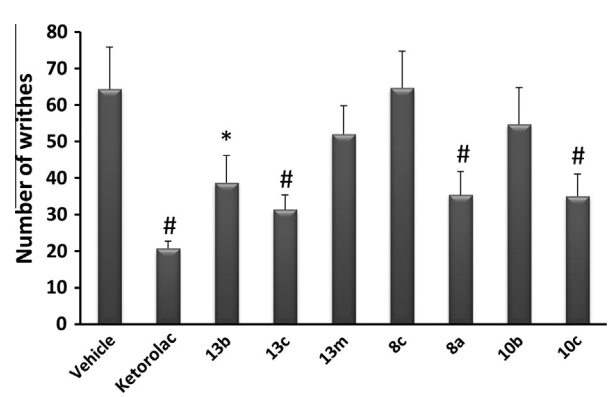

Fig. 4. Results of acetic acid-induced writhing test. Data are mean ± SD ($N = 6–8$). $^{*}P < 0.05$, $^{\#}P < 0.01$ represents significant change in number of writhes compared to vehicle-treated group.

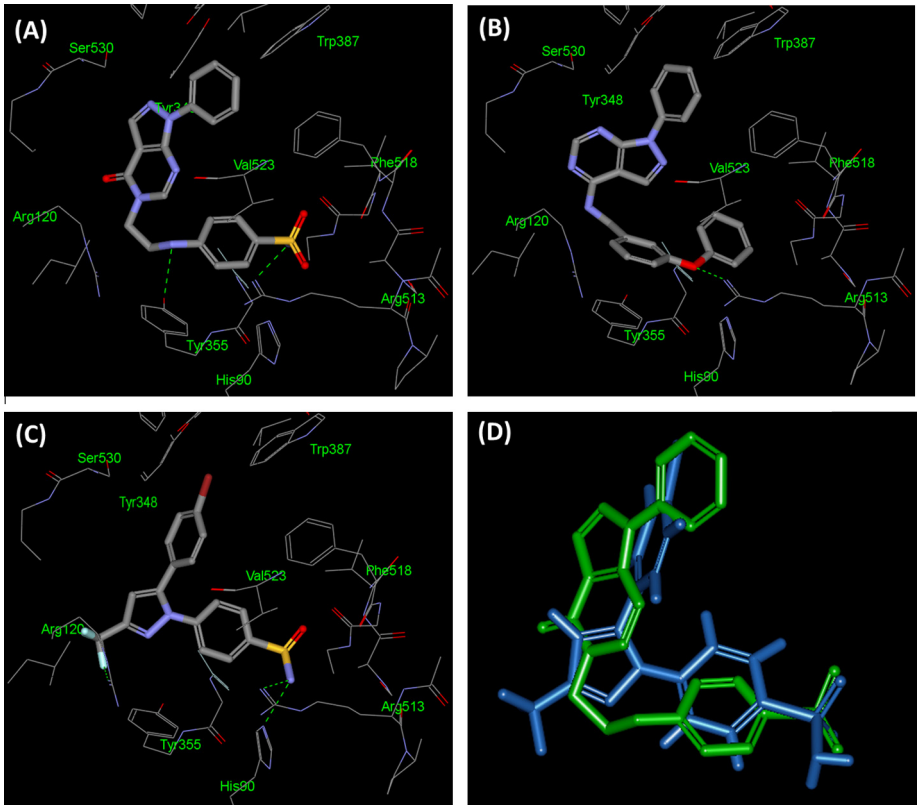

Fig. 5. (A) Docking and binding mode of compound **8a** into COX-2 active site (PDB code: 1CX2). (B) Docking and binding mode of compound **10c** into the same COX-2 binding pocket. (C) X-ray crystallographic structure of bromocelecoxib analog, **SC-558** co-crystallized within COX-2 active site (PDB code: 1CX2). (D) The superposition of the docked poses **8a** (green) and the co-crystallized **SC-558** (blue) within active site of COX-2. Hydrogen bonds are represented by dashed green lines. All hydrogens are removed for the purposes of clarity. (For interpretation of the references to colour in this figure legend, the reader is referred to the web version of this article.)

of the oxygen in **13a** with Arg120 which is essential for COX-1 affinity and selectivity.

Interestingly, docking of compound **13b** into both COX-1 and COX-2 active sites explained the non-selectivity and affinity of this compound for both COX subtypes where it could successfully bind to both active sites, Fig. 7. As mentioned, the absence of the side pocket in COX-1 forced the compound to have a longitudinal binding pattern similar to the former selective compounds **8d** and **13a**. On the contrary, the COX-2 side corridor accommodated the bulky hexylpiperazine fragment by forming an additional H-bond with Tyr355 residue and an electrostatic interaction with Arg513.

Similarly, the active compounds **10c** and **11** were docked into the active site of the X-ray structure of iNOS complexed with the selective inhibitor AR-C120011 (pdb code: **3E65**). The two compounds adopted a position and orientation similar to that of the selective spiro inhibitor, AR-C120011, Fig. 8. The reported extending pocket exposed from rotations of Gln257, Arg260 and other residues (Garcin et al., 2008) can explain the accommodation of iNOS binding site for bulky phenoxy fragment of **10c** and the phenyl ring of **11** and their enhanced inhibitory activity. Apparently, the two docked compounds showed a common critical hydrophobic stacking interaction between the phenyl ring linked to the

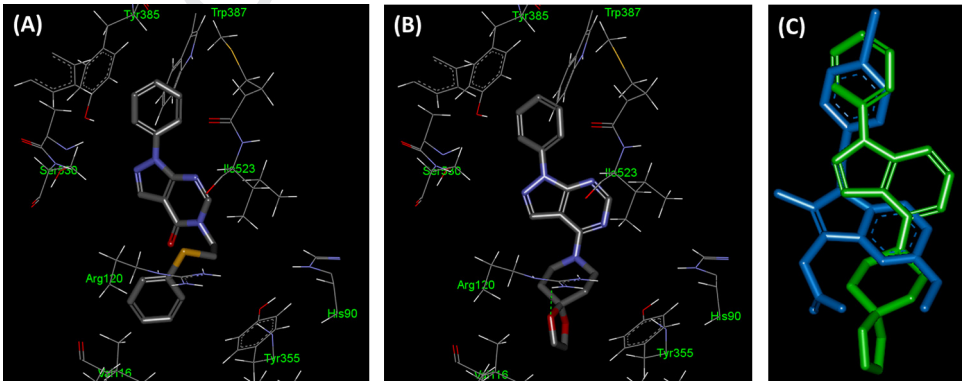

Fig. 6. (A) Docking and binding mode of compound **8d** into COX-1 active site (PDB code: 1PGF). (B) Docking and binding mode of compound **13a** into the same COX-1 binding pocket. (C) The superposition of the docked poses AH-6 (green) and the co-crystallized Iodoindomethacin, **IMM** (blue) within active site of COX-1. Hydrogen bonds are represented by dashed green lines. All hydrogens are removed for the purposes of clarity. (For interpretation of the references to colour in this figure legend, the reader is referred to the web version of this article.)

Please cite this article in press as: Abdelazeem, A.H., et al. Novel pyrazolopyrimidine derivatives targeting COXs and iNOS enzymes; design, synthesis and biological evaluation as potential anti-inflammatory agents. Eur. J. Pharm. Sci. (2014), http://dx.doi.org/10.1016/j.ejps.2014.05.025

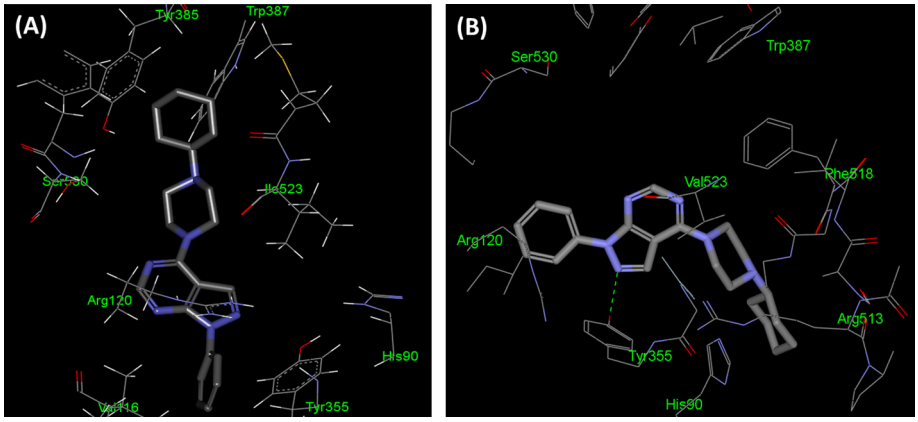

Fig. 7. (A) Docking and binding mode of compound **13b** into COX-1 active site (PDB code: 1PGF). (B) Docking and binding mode of the same compound into COX-2 binding pocket (PDB code: 1CX2). Hydrogen bonds are represented by dashed green lines. All hydrogens are removed for the purposes of clarity. (For interpretation of the references to colour in this figure legend, the reader is referred to the web version of this article.)

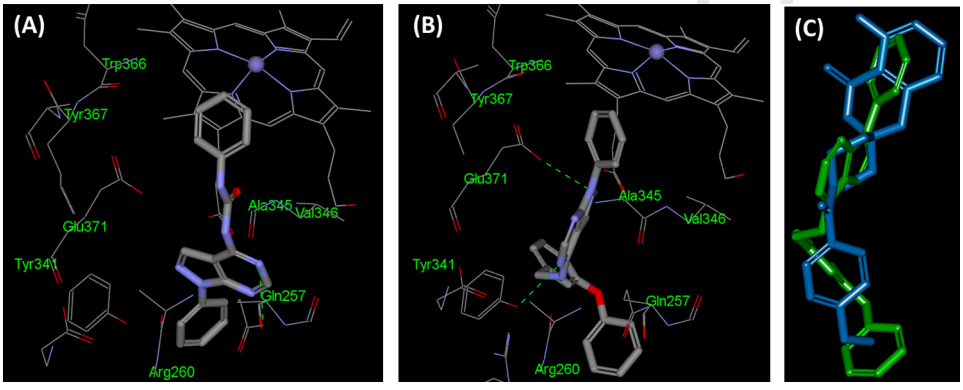

Fig. 8. (A) Docking and binding mode of compound **11** into iNOS active site (PDB code: 3E65). (B) Docking and binding mode of compound **10c** into the same iNOS binding pocket. (C) The superposition of the docked poses **10c** (green) and the co-crystallized spiro ligand, **AR-C120011** (blue) within the active site of iNOS. Hydrogen bonds are represented by dashed green lines. All hydrogens are removed for the purposes of clarity. (For interpretation of the references to colour in this figure legend, the reader is referred to the web version of this article.)

pyrazole moiety in **10c** and phenyl ring attached to the urea group in **11** and heme within the binding pocket of iNOS. An additional hydrogen bond tethered the nitrogen of the pyrimidine heterocycle in **11** to Gln257 amino acid, as shown in Fig. 8(**A**). It could also be appreciated from Fig. 8(B) how compound **10c** formed two hydrogen-bonding interactions with Glu371 and Tyr341 residue as well. These results indicated that hydrophobic aromatic stacking, as well as hydrogen bonds within the active sites of COXs and iNOS significantly contribute to the binding modes of these compounds and their activity.

3. Conclusion

In this study, two sets of compounds from 4-substituted-1-phenyl-pyrazolo[3,4-*d*]pyrimidine and 5-substituted-1-phenyl-pyrazolo[3,4-*d*]pyrimidin-4-one were synthesized and evaluated for their anti-inflammatory potential. The newly synthesized compounds were screened *in vitro* against four anti-inflammatory targets; COX subtypes (COX-1 and COX-2), iNOS and NF-kB. In COXs inhibitory assays, three compounds **8a**, **10c** and **13c** showed significant inhibition and good selectivity against COX-2. On the contrary, compounds **8d** and **13a** exhibited good selectivity against COX-1 with moderate inhibition. Moreover, compound **13c** was a non-selective ligand against both COXs. On the other hand, compounds **8c**, **8g**, **10c** and **11** were the most active ligands against iNOS with IC_{50} values of 0.27, 0.24, 0.30 and 0.22 μM respectively. Meanwhile, most of the tested compounds were devoid of inhibitory activity against NF-kB except compounds **8e** and **13d** which showed moderate inhibition with IC_{50} values of 5.3 and 2.8 μM respectively. In addition, most of the compounds were not cytotoxic, up to 25 μg/ml, on a panel of normal and cancer cell lines as well. Interestingly, the docking results were in agreement with that of the inhibitory activity against the COX subtypes and iNOS enzymes where the important structural features and proper orientations and binding modes required for activity were determined. *In vivo* anti-inflammatory and analgesic studies revealed that compounds **8a**, **10c** and **13c** have significant anti-inflammatory and analgesic activities comparable to that of ketorolac. It was noticed that the results of *in vivo* studies were consistent with that of *in vitro* COXs and iNOS assays. In conclusion, compounds **8a**, **10c** and **13c** showed a dual inhibition for both COX-2 and iNOS which appears to be a valid strategy for further development of novel anti-inflammatory drugs.

4. Experimental protocols

4.1. Chemistry

Reagents and starting materials were obtained from commercial suppliers and were used without purification. Precoated silica gel GF Uniplates from Analtech were used for thin-layer chromatography (TLC). Column chromatography was done on silica gel 60 (Sorbent Technologies). Melting points (m.p.) were uncorrected

and were carried out by open capillary tube method using IA 9100MK-Digital Melting Point Apparatus. ^{1}H and ^{13}C NMR spectra were obtained on a Bruker APX400 at 400 and 100 MHz, respectively. Chemical shifts were reported on the δ scale and were related to that of the solvent and *J* values are given in Hz. The mass spectra (MS) were recorded on a Waters Acquity Ultra Performance LC with ZQ detector in ESI mode. The infrared spectra IR were obtained from PerkinElmer Spectrum 100FT-IR Spectrometer. Elemental analyses (C, H, N) were recorded on an elemental analyzer, Perkin-Elmer CHN/SO series II Analyzer. Chemical names were generated using ChemDraw Ultra (Cambridge Soft, version 11.0.1).

*5-Amino-1-phenyl-1H-pyrazole-4-carbonitrile (**5**).* Ethoxymethylenemalononitrile (20.3 gm, 0.17 mol) was added slowly with shaking to phenylhydrazine (18 gm, 0.17 mol) in 40 mL absolute ethanol at room temperature. After the addition was completed, the solution was carefully heated to boiling for about one hour. The reaction mixture was then set aside overnight in the refrigerator. The product was filtered, washed with a little ether and further purified by recrystallization from ethanol to give white crystals, m.p. 140 °C. ^{1}H NMR (400 MHz, DMSO-d_6) δ 3.52 (s, 2H, N$\underline{H_2}$), 7.22–7.29 (m, 1H), 7.43–7.55 (m, 2H), 8.15–8.21 (d, *J* = 8.47 Hz, 2H), 8.40 (s, 1H). ^{13}C NMR (101 MHz, DMSO) δ 158.77, 157.10, 153.71, 139.44, 129.48, 126.39, 120.96, 101.91. MS (EI) *m/z* 185.18 (M^{+}+1).

*1-Phenyl-1H-pyrazolo[3,4-d]pyrimidin-4(5H)-one (**6**).* Compound **5** (3.44 g, 0.01 mol) was refluxed in formic acid (30 mL, 85%) for 6 h. The reaction mixture was cooled and poured into water. The formed solid was filtered off, dried, and recrystallized from dioxane to give compound **6** (75%) as a white solid, m.p. 265–267 °C. ^{1}H NMR (400 MHz, DMSO-d_6) δ 7.37 (t, *J* = 4.34 Hz, 1H), 7.53 (t, *J* = 8.31 Hz, 2H), 8.02 (d, *J* = 7.85 Hz, 2H), 8.18 (s, 1H), 8.31 (s, 1H), 12.44 (s, 1H, N$\underline{H}$). ^{13}C NMR (101 MHz, DMSO) δ 157.65 (C=O), 152.27, 149.20, 138.66, 136.41, 129.61, 127.52, 122.14, 108.06. MS (EI) *m/z* 212.20 (M^{+}).

*5-(2-Bromoethyl)-1-phenyl-1H-pyrazolo[3,4-d]pyrimidin-4(5H)-one (**7**).* A solution of compound **6** (3 g, 14.2 mmol) in dry DMF (20 mL) was cooled to 0 °C. Sodium hydride (65% dispersion in oil, 0.55 g, 16.25 mmol) was added, and the solution was stirred for 30 min at 0 °C. 1,2 Dibromoethane (13.18 g, 70.5 mmol) was added, the ice bath was removed, and the solution was stirred for 4 h at room temperature. The mixture was poured onto H_2O and washed with ethyl acetate (5 × 40 mL). The organic layer was washed with H_2O and brine. The organic layer was then dried over Na_2SO_4 and filtered, and the solvent was removed in vacuo to give compound **7** as yellowish white solid (63%). mp 125–127 °C. ^{1}H NMR (400 MHz, DMSO-d_6) δ 3.83 (t, *J* = 7.24 Hz, 2H), 4.42 (t, *J* = 7.32 Hz, 2H), 7.37–7.41 (m, 1H), 7.55 (t, *J* = 7.79 Hz, 2H), 8.02 (d, *J* = 7.71 Hz, 2H), 8.37 (s, 1H), 8.52 (s, 1H). ^{13}C NMR (101 MHz, DMSO) δ 156.67 (C=O), 151.77, 151.58, 138.46, 136.56, 129.67, 127.63, 122.06, 107.19, 47.39, 31.35. MS (EI) *m/z* 319.06 (M^{+}+1). Anal. Calcd. for $C_{13}H_{11}BrN_4O$: C, 48.92; H, 3.47.; N, 17.55. Found: C, 49.27; H, 3.41.; N, 17.54.

***General procedure A**. Synthesis of compounds (**8a–f**). 4-((2-(4-oxo-1-phenyl-1H-pyrazolo[3,4-d]pyrimidin-5(4H)-yl)ethyl)amino)benzenesulfonamide (**8a**).* K_2CO_3 (0.74 g, 5.33 mmol) and 4-sulfanilamide (0.31 g, 1.78 mmol) were added, while stirring, to a solution of compound **7** (0.56 g, 1.78 mmol) in anhydrous DMF (15 mL). The reaction mixture was heated at 60 °C for 2 h. After cooling, the mixture was poured onto H_2O (100 mL), extracted with ethyl acetate (3 × 40 mL), washed with saturated aqueous NaCl and dried over Na_2SO_4. The solvent was removed in vacuo, and the residue was chromatographed on a silica gel column using methylene chloride/methanol (9:1) as the eluent to afford 4-((2-(4-oxo-1-phenyl-1*H*-pyrazolo[3,4-*d*]pyrimidin-5(4*H*)-yl)ethyl)amino)benzenesulfonamide **8a** (71%) as a white solid. mp 215–217 °C. ^{1}H NMR (400 MHz, DMSO-d_6) δ 3.67 (t, *J* = 4.18 Hz, 2H), 4.19 (t, *J* = 4.36 Hz, 2H), 4.41 (s, 1H, N$\underline{H}$), 5.01 (s, 2H, N$\underline{H_2}$), 6.58–6.64 (m, 4H), 7.41–7.47 (m, 3H), 7.99 (d, *J* = 8.17 Hz, 2H), 8.53 (s, 1H), 8.77 (s, 1H). ^{13}C NMR (101 MHz, DMSO) δ 152.66, 152.33, 152.13, 140.18, 137.90, 130.41, 129.75, 128.03, 127.87, 122.78, 113.14, 112.98, 103.94, 57.61, 52.02. MS (EI) *m/z* 411.17 (M^{+}+1). Anal. Calcd. for $C_{19}H_{18}N_6O_3S$: C, 55.60; H, 4.42; N, 20.48. Found: C, 55.67; H, 4.36; N, 20.08.

*1-Phenyl-5-(2-(pyrrolidin-1-yl)ethyl)-1H-pyrazolo[3,4-d]pyrimidin-4(5H)-one (**8b**).* General Procedure **A**, yield 67%, Creamy white solid, mp 153–155 °C. ^{1}H NMR (400 MHz, DMSO-d_6) δ 1.63 (t, *J* = 4.45 Hz, 4H), 2.47 (t, *J* = 8.17 Hz, 4H), 2.68 (t, *J* = 8.11 Hz, 2H), 4.08 (t, *J* = 4.05 Hz, 2H), 7.37 (t, *J* = 8.55 Hz, 1H), 7.54 (t, *J* = 8.70 Hz, 2H), 8.02 (d, *J* = 4.24 Hz, 2H), 8.33 (s, 1H), 8.40 (s, 1H). ^{13}C NMR (101 MHz, DMSO) δ 156.72 (C=O), 151.95, 151.66, 138.57, 136.49, 129.66, 127.51, 121.97, 107.30, 54.54, 54.02, 44.67, 23.65. MS (EI) *m/z* 310.03 (M^{+}+1). Anal. Calcd. for $C_{17}H_{19}N_5O$: C, 66.00; H, 6.19; N, 22.64. Found: C, 66.37; H, 5.82; N, 22.91.

*5-(2-(Azepan-1-yl)ethyl)-1-phenyl-1H-pyrazolo[3,4-d]pyrimidin-4(5H)-one (**8c**).* General Procedure **A**, yield 67%, white solid, mp 105–107 °C. ^{1}H NMR (400 MHz, DMSO-d_6) δ 1.42 (s, 4H), 2.50–264 (m, 4H), 2.72 (t, *J* = 4.77 Hz, 2H), 3.40 (t, *J* = 16.53 Hz, 4H), 4.04 (t, *J* = 8.81 Hz, 2H), 7.34–7.40 (m, 1H), 7.55 (t, *J* = 7.93 Hz, 2H), 8.04 (d, *J* = 4.04 Hz, 2H), 8.34 (s, 1H), 8.38 (s, 1H). ^{13}C NMR (101 MHz, DMSO) δ 156.76, 152.07, 151.72, 138.61, 136.46, 129.66, 127.46, 121.89, 107.24, 56.28, 55.46, 44.11, 28.50, 26.87. MS (EI) *m/z* 338.10 (M^{+}+1). Anal. Calcd. for $C_{19}H_{23}N_5O$: C, 67.63; H, 6.87; N, 20.76. Found: C, 68.31; H, 6.35; N, 20.71.

*1-Phenyl-5-(2-(phenylthio)ethyl)-1H-pyrazolo[3,4-d]pyrimidin-4(5H)-one (**8d**).* General Procedure **A**, yield 67%, white solid, mp 108–110 °C. ^{1}H NMR (400 MHz, DMSO-d_6) δ 3.66 (t, *J* = 4.28 Hz, 2H), 4.08 (t, *J* = 8.28 Hz, 2H), 7.32–7.41 (m, 3H), 7.98–8.05 (m, 5H), 8.37 (d, *J* = 4.26 Hz, 2H), 8.43 (s, 1H), 8.52 (s, 1H). ^{13}C NMR (101 MHz, DMSO) δ 156.88 (C = O), 156.68, 152.24, 151.77, 139.36, 138.46, 134.30, 129.80, 129.68, 125.94, 122.07, 121.93, 107.19, 47.40, 31.35. MS (EI) *m/z* 349.39 (M^{+}+1). Anal. Calcd. for $C_{19}H_{16}N_4OS$: C, 65.50; H, 4.63; N, 16.08. Found: C, 65.54; H, 4.35; N, 15.91.

*3-(2-(4-oxo-1-Phenyl-1H-pyrazolo[3,4-d]pyrimidin-5(4H)-yl)ethyl) benzo[d]thiazol-2(3H)-one (**8e**).* General Procedure **A**, yield 67%, white solid, mp 211–213 °C. ^{1}H NMR (400 MHz, DMSO-d_6) δ 3.63 (t, *J* = 27.12 Hz, 2H), 4.31 (t, *J* = 17.15 Hz, 2H), 7.15 (t, *J* = 7.58 Hz, 1H), 7.27–7.40 (m, 3H), 7.50–7.60 (m, 3H), 7.94 (d, *J* = 8.20 Hz, 2H), 8.25 (s, 1H), 8.29 (s, 1H). ^{13}C NMR (101 MHz, DMSO) δ 169.76 (S-C=O), 157.06 (C=O), 151.46, 151.35, 138.34, 136.91, 136.49, 129.72, 127.69, 127.03, 123.76, 123.35, 122.01, 121.84, 111.45, 106.98, 43.79, 41.56. MS (EI) *m/z* 390.02 (M^{+}+1). Anal. Calcd. for $C_{20}H_{15}N_5O_2S$: C, 61.68; H, 3.88; N, 17.98. Found: C, 61.41; H, 3.64; N, 17.91.

*5-(2-(Bis(2-hydroxyethyl)amino)ethyl)-1-phenyl-1H-pyrazolo[3,4-d]pyrimidin-4(5H)-one (**8f**).* General Procedure **A**, yield 67%, light brown solid, mp 121–123 °C. MS (EI) *m/z* 344.17 (M^{+}+1). It was used directly for the preparation of compound **8g**.

*5-(2-(Bis(2-chloroethyl)amino)ethyl)-1-phenyl-1H-pyrazolo[3,4-d]pyrimidin-4(5H)-one (**8g**).* A mixture of compound **8f** (0.4 g, 1.17 mmol) in thionyl chloride (3 mL) and dry benzene (10 mL) was heated gently under reflux until a homogenous solution was obtained, then for a further one hour. The solution was evaporated to dryness under vacuum to remove excess thionyl chloride. The residue was azeotroped with dry benzene (3 × 5 mL) where the last traces of thionyl chloride were removed. The residue obtained was purified by flash column chromatography (SiO_2) using methylene chloride/methanol (9.5:0.5) as eluent to give 0.25 g (62%) of compound **8g** as a yellowish white solid. ^{1}H NMR (400 MHz, DMSO-d_6) δ 3.41–3.57 (m, 6H), 3.97 (t, *J* = 8.15 Hz, 2H), 4.35–4.41 (m, 4H), 7.40 (t, *J* = 8.36 Hz, 1H), 7.56 (t, *J* = 7.84 Hz, 2H), 8.02 (d, *J* = 8.23 Hz, 2H), 8.38 (s, 1H), 8.51 (s, 1H). ^{13}C NMR (101 MHz, DMSO) δ 156.74 (C=O), 151.97, 151.60, 138.46, 136.56, 129.70, 127.67, 122.12, 107.19, 47.54, 47.48, 42.80, 42.75. MS (EI) *m/z* 380.12

(M^++1). Anal. Calcd. for $C_{17}H_{19}Cl_2N_5O$: C, 53.69; H, 5.04; N, 18.42. Found: C, 53.48; H, 4.93; N, 18.14.

*1-Phenyl-1H-pyrazolo[3,4-d]pyrimidin-4-amine (**9**).* 5-amino-1-phenyl-1*H*-pyrazole-4-carbonitrile **5** (3.5 gm, 19 mmol) was added to formamide (20 mL). The solution was refluxed for 4 h and allowed to cool. The reaction mixture was poured onto water and the product was filtered and recrystallized from dioxane to give a light brown solid of compound **9** (56%). ^{1}H NMR (400 MHz, DMSO-d_6) δ 7.29 (t, *J* = 7.43 Hz, 1H), 7.51 (t, *J* = 5.68 Hz, 2H), 7.98 (br. s, 2H, N$\underline{H}_2$), 8.20 (d, *J* = 7.27 Hz, 2H), 8.34 (s, 1H), 8.40 (s, 1H). ^{13}C NMR (101 MHz, DMSO) δ 158.89, 157.23, 153.83, 139.56, 134.62, 129.60, 126.51, 121.08, 102.03. MS (EI) *m*/*z* 212.27 (M^++1).

***General procedure B**. Synthesis of compounds (**10a–c**). N-(furan-3-ylmethyl)-1-phenyl-1H-pyrazolo[3,4-d]pyrimidin-4-amine (**10a**).* 1-phenyl-1*H*-pyrazolo[3,4-*d*]pyrimidin-4-amine, **9** (1.0 g, 4.73 mmol) and 3-furaldehyde (0.45 g, 4.73 mmol) were mixed in 1,2-dichloroethane (20 mL) and then treated with sodium triacetoxyborohydride (1.5 g, 6.62 mmol) and acetic acid (0.28 g, 4.73 mmol). The mixture was stirred at room temperature for 24 h until the reactants were consumed. The reaction mixture was quenched by 1 N NaOH, and the product was extracted with CH_2Cl_2. The organic extract was washed with brine and dried (Na_2SO_4). The solvent was evaporated and the residue obtained was purified by flash column chromatography (SiO_2) using methylene chloride/methanol (9.5:0.5) as eluent to give compound **10a** as a white solid (82%). mp 143–145 °C. ^{1}H NMR (400 MHz, DMSO-d_6) δ 3.48 (s, 1H, N$\underline{H}$), 3.84 (s, 2H, C$\underline{H}_2$), 6.74–6.77 (dd, *J* = 4.52, 7.46 Hz, 1H), 6.89 (d, *J* = 8.31 Hz, 1H), 7.43 (t, *J* = 4.24 Hz, 1H), 7.61–7.68 (m, 3H), 8.25 (d, *J* = 4.35, 2H), 8.48 (s, 1H), 8.64 (s, 1H). ^{13}C NMR (101 MHz, DMSO) δ 158.64, 156.81, 155.63, 154.11, 147.88, 139.00, 135.37, 129.33, 126.55, 121.36, 113.29, 107.03, 101.52, 43.89. MS (EI) *m*/*z* 292.16 (M^++1). Anal. Calcd. for $C_{16}H_{13}N_5O$: C, 65.97; H, 4.50; N, 24.04. Found: C, 65.84; H, 4.12; N, 23.83.

*N-(4-Nitrobenzyl)-1-phenyl-1H-pyrazolo[3,4-d]pyrimidin-4-amine (**10b**).* General Procedure **B**, yield 67%, white solid, mp 81–84 °C. ^{1}H NMR (400 MHz, DMSO-d_6) δ 4.02 (s, 2H, C$\underline{H}_2$), 4.76 (s, 1H, N$\underline{H}$), 6.79 (d, *J* = 4.52, 2H), 6.97 (d, *J* = 4.31 Hz, 2H), 7.27 (t, *J* = 8.24 Hz, 1H), 7.46 (t, *J* = 8.21 Hz, 2H), 8.10 (d, *J* = 4.35, 2H), 8.31 (s, 1H), 8.51 (s, 1H). ^{13}C NMR (101 MHz, DMSO) δ 155.92, 154.58, 153.34, 148.48, 138.14, 134.09, 128.24, 127.99, 125.52, 121.86, 120.47, 115.83, 100.61, 46.65. MS (EI) *m*/*z* 347.22 (M^++1). Anal. Calcd. for $C_{18}H_{14}N_6O_2$: C, 62.42; H, 4.07; N, 24.27. Found: C, 63.10; H, 3.98; N, 24.13.

*N-(3-Phenoxybenzyl)-1-phenyl-1H-pyrazolo[3,4-d]pyrimidin-4-amine (**10c**).* General Procedure **B**, yield 67%, white solid, mp 230–232 °C. ^{1}H NMR (400 MHz, DMSO-d_6) δ 3.55 (s, 1H, N$\underline{H}$), 4.85 (s, 2H), 6.95–7.00 (m, 3H), 7.09–7.13 (m, 2H), 7.34–7.39 (m, 6H), 8.10 (d, *J* = 4.35 Hz, 2H), 8.44 (s, 1H), 8.68 (s, 1H). ^{13}C NMR (101 MHz, DMSO) δ 157.27, 157.10, 156.82, 145.46, 135.42, 130.58, 130.46, 130.06, 129.70, 127.37, 123.97, 123.09, 121.80, 119.13, 118.28, 117.76, 117.25, 116.69, 102.13, 44.48. MS (EI) *m*/*z* 394.19 (M^++1). Anal. Calcd. for $C_{24}H_{19}N_5O$: C, 73.27; H, 4.87; N, 17.80. Found: C, 73.25; H, 4.81; N, 17.96.

*1-Phenyl-3-(1-phenyl-1H-pyrazolo[3,4-d]pyrimidin-4-yl)urea (**11**).* A mixture of 1-phenyl-1*H*-pyrazolo[3,4-*d*]pyrimidin-4-amine, **9** (1.0 g, 4.73 mmol) in methylene chloride (25 mL), phenylisocyanate (0.56 g, 4.73 mmol.) and few drops of triethylamine were stirred and left overnight. The reaction mixture was then evaporated and the residue was dissolved in acetone, concentrated; set aside where the solid obtained is collected, dried & recrystallized from ethanol-acetone to give a white crystals from compound **11** (74%). mp 187–189 °C. ^{1}H NMR (400 MHz, DMSO-*d*6) δ 5.52 (s, 2H, 2N$\underline{H}$), 7.00–7.28 (m, 3H), 7.30 (t, *J* = 8.31 Hz, 1H), 7.47–7.57 (m, 3H), 7.72 (d, *J* = 8.21 Hz, 1H), 8.14 (d, *J* = 8.35, 2H), 8.32 (s, 1H), 8.49 (s, 1H). ^{13}C NMR (101 MHz, DMSO) δ 159.04 (C=O), 155.78, 154.67, 153.18, 149.75, 137.99, 134.30, 128.37, 128.34, 125.62, 120.43, 118.33, 114.61, 100.47. MS (EI) *m*/*z* 331.24 (M^++1). Anal. Calcd.. for $C_{18}H_{14}N_6O$: C, 65.44; H, 4.27; N, 25.44. Found: C, 65.51; H, 4.21; N, 25.49.

*4-Chloro-1-phenyl-1H-pyrazolo[3,4-d]pyrimidine (**12**).* 1-Phenyl-1*H*-pyrazolo[3,4-*d*]pyrimidin-4(5*H*)-one, **6** (10 g) was suspended in phosphorus oxychloride (50 mL) containing few drops of DMF. The mixture was refluxed for two hours. The excess phosphorus oxychloride was removed from the clear yellow solution under reduced pressure and the residue was then poured slowly with vigorous stirring onto ice water (250 mL). The mixture was allowed to stand for 30 min, and the white suspension was extracted with methylene chloride (3 × 60 mL.). The solvent was evaporated and the residue obtained was dried and purified by flash column chromatography (SiO_2) using CH_2Cl_2/CH_3OH (9.5:0.5) as eluent to give the chloro-derivative **12** as a yellow solid (92%), m.p. to 198–199. ^{1}H NMR (400 MHz, DMSO-d_6) δ 7.37 (t, *J* = 8.42 Hz, 1H), 7.52 (t, *J* = 7.30 Hz, 2H), 8.00 (d, *J* = 4.47 Hz, 2H), 8.32 (s, 1H), 8.55 (s, 1H). ^{13}C NMR (101 MHz, DMSO) δ 156.56, 151.70, 151.59, 138.49, 136.59, 129.60, 127.54, 122.05, 107.36. MS (EI) *m*/*z* 231.11 (M^++1).

***General procedure C**. Synthesis of compounds (**13a–m**). 8-(1-phenyl-1H-pyrazolo[3,4-d]pyrimidin-4-yl)-1,4-dioxa-8-azaspiro[4.5] decane (**13a**).* A mixture of 4-chloro-1-phenyl-1*H*-pyrazolo[3,4-*d*]pyrimidine **12** (1 g, 4.34 mmol) and 1,4-dioxa-8-azaspiro[4.5] decane (0.62 g, 4.34 mmol) in 2-propanol (30 mL) or 95% ethanol for other amines was refluxed for two hour. The white solid formed in the hot solution was collected after cooling and further recrystallized from ethanol yielded white crystals of compound **13a** (67%). mp 170–172 °C. ^{1}H NMR (400 MHz, Chloroform-*d*) δ 1.88 (t, *J* = 7.99 Hz, 4H), 4.03 (s, 4H), 4.11 (t, *J* = 8.21 Hz, 4H), 7.31–7.35 (m, 1H), 7.50–7.54 (m, 2H), 8.11–8.14 (m, 3H), 8.45 (s, 1H). ^{13}C NMR (101 MHz, $CDCl_3$) δ 156.75, 155.63, 154.39, 138.87, 133.78, 129.08, 126.64, 122.05, 106.87, 101.67, 64.57, 43.75, 34.93. MS (EI) *m*/*z* 338.17 (M^++1). Anal. Calcd. for $C_{18}H_{19}N_5O_2$: C, 64.08; H, 5.68; N, 20.76; Found: C, 64.12; H, 5.32; N, 20.47.

*4-(4-Cyclohexylpiperazin-1-yl)-1-phenyl-1H-pyrazolo[3,4-d]pyrimidine (**13b**).* General Procedure **C**, yield 67%, white solid, mp 109–111 °C. ^{1}H NMR (400 MHz, Chloroform-*d*) δ 1.09–1.23 (m, 5H), 1.54–1.94 (m, 5H), 2.22–2.41 (m, 1H), 2.72 (t, *J* = 8.04 Hz, 4H), 4.00 (t, *J* = 8.06 Hz, 4H), 7.26–7.33 (m, 1H), 7.47–7.52 (m, 2H), 8.10–8.12 (m, 3H), 8.43 (s, 1H). ^{13}C NMR (101 MHz, $CDCl_3$) δ 156.99, 155.56, 154.34, 138.88, 133.88, 129.07, 126.61, 122.02, 101.69, 63.57, 48.74, 48.73, 28.90, 26.23, 25.78. MS (EI) *m*/*z* 363.21 (M^++1). Anal. Calcd. for $C_{21}H_{26}N_6$: C, 69.58; H, 7.23; N, 23.19. Found: C, 69.81; H, 7.07; N, 23.42.

*4-(4-(4-Fluorophenyl)piperazin-1-yl)-1-phenyl-1H-pyrazolo[3,4-d] pyrimidine (**13c**)* (Natarajan et al., 2005). General Procedure **C**, yield 67%, white solid, mp 140–142 °C. ^{1}H NMR (400 MHz, DMSO-d_6) δ 3.24 (t, *J* = 4.21 Hz, 4H), 4.07 (t, *J* = 4.11 Hz, 4H), 6.93–6.97 (dd, *J* = 4.59, 9.02 Hz, 2H), 7.02–7.08 (m, 2H), 7.31–7.35 (m, 1H), 7.52 (t, *J* = 7.85 Hz, 2H), 8.17 (d, *J* = 8.00 Hz, 2H), 8.37 (s, 1H), 8.54 (s, 1H). ^{13}C NMR (101 MHz, DMSO) δ 156.43, 155.34–155.29 (d, *J* = 5.05), 153.87, 147.41, 138.70, 134.90, 131.19, 129.03, 126.27, 121.10, 117.30–117.22 (d, *J* = 8.08), 115.49–115.27 (d, *J* = 22.22), 101.15, 48.61, 48.56. MS (EI) *m*/*z* 375.22 (M^++1). Anal. Calcd. for $C_{21}H_{19}FN_6$: C, 67.37; H, 5.11; N, 22.45. Found: C, 67.41; H, 4.94; N, 22.12.

*1-Phenyl-4-(4-phenylpiperazin-1-yl)-1H-pyrazolo[3,4-d]pyrimidine (**13d**).* General Procedure **C**, yield 67%, white solid, mp 118–120 °C. ^{1}H NMR (400 MHz, DMSO-d_6) δ 3.34 (t, *J* = 8.3 Hz, 4H), 4.11 (t, *J* = 4.2 Hz, 4H), 6.80 (t, *J* = 8.22 Hz, 1H), 6.90–7.01 (m, 2H), 7.22–7.36 (m, 3H), 7.50–7.57 (m, 2H), 8.18 (d, *J* = 8.2 Hz, 2H), 8.40 (s, 1H), 8.58 (s, 1H). ^{13}C NMR (101 MHz, DMSO) δ 156.93, 155.82, 154.33, 150.91, 139.14, 135.46, 129.52, 129.50, 126.77, 121.59, 119.48, 115.76, 101.62, 48.12, 48.08. MS (EI) *m*/*z* 357.22 (M^++1). Anal. Calcd. for $C_{21}H_{20}N_6$: C, 70.77; H, 5.66; N, 23.58. Found: C, 70.55; H, 5.93; N, 23.61.

Please cite this article in press as: Abdelazeem, A.H., et al. Novel pyrazolopyrimidine derivatives targeting COXs and iNOS enzymes; design, synthesis and biological evaluation as potential anti-inflammatory agents. Eur. J. Pharm. Sci. (2014), http://dx.doi.org/10.1016/j.ejps.2014.05.025

*1-Phenyl-4-(4-(4-(trifluoromethyl)phenyl)piperazin-1-yl)-1H-pyrazolo[3,4-d]pyrimidine (**13e**).* General Procedure **C**, yield 67%, white solid, mp 210–212 °C. ^{1}H NMR (400 MHz, DMSO-d_6) δ 3.61 (t, J = 4.21, 4H), 4.20 (t, J = 8.34, 4H), 7.04 (d, J = 8.54 Hz, 2H), 7.36–7.41 (m, 1H), 7.52–7.58 (m, 4H), 8.09–8.12 (m, 2H), 8.45 (s, 1H), 8.66 (s, 1H). ^{13}C NMR (101 MHz, DMSO) δ 154.95, 153.46, 153.17, 152.56, 138.62, 136.26, 129.63, 127.35, 126.75–126.71 (d, J = 4.04), 124.12, 122.02, 118.23–117.91 (d, J = 32.3), 113.78, 101.66, 45.86, 45.84. MS (EI) m/z 425.20 (M^++1). Anal. Calcd. for $C_{22}H_{19}F_3N_6$: C, 62.26; H, 4.51; N, 19.80. Found:. C, 62.51; H, 4.31; N, 20.14.

*1-Phenyl-4-(4-(pyridin-2-yl)piperazin-1-yl)-1H-pyrazolo[3,4-d]pyrimidine (**13f**).* General Procedure **C**, yield 67%, white solid, mp 138–140 °C. ^{1}H NMR (400 MHz, DMSO-d_6) δ 3.74 (t, J = 8.18 Hz, 4H), 4.08 (t, J = 4.44 Hz, 4H), 6.64–6.67 (dd, J = 4.84, 7.07 Hz, 1H), 6.79 (d, J = 8.56 Hz, 1H), 7.33 (t, J = 4.37 Hz, 1H), 7.51–7.58 (m, 3H), 8.13–8.18 (m, 3H), 8.38 (s, 1H), 8.54 (s, 1H). ^{13}C NMR (101 MHz, DMSO) δ 158.80, 156.97, 155.79, 154.27, 148.04, 139.16, 138.06, 135.53, 129.49, 126.71, 121.52, 113.45, 107.19, 101.68, 44.05, 43.99. MS (EI) m/z 358.30 (M^++1). Anal. Calcd. for $C_{20}H_{19}N_7$: C, 67.21; H, 5.36; N, 27.43. Found: C, 67.08; H, 5.70; N, 27.19.

*4-(4-(4-Fluorobenzyl)piperazin-1-yl)-1-phenyl-1H-pyrazolo[3,4-d]pyrimidine (**13g**).* General Procedure **C**, yield 67%, white solid, mp 182–184 °C. ^{1}H NMR (400 MHz, DMSO-d_6) δ 3.14 (t, J = 4.45 Hz, 4H), 3.91 (t, J = 4.32 Hz, 4H), 4.61 (s, 2H, C$\underline{H_2}$), 6.73–6.83 (m, 2H), 6.84–6.88 (m, 2H), 7.11–7.15 (m, 1H), 7.32 (t, J = 7.85 Hz, 2H), 7.97 (d, J = 8.00 Hz, 2H), 8.17 (s, 1H), 8.34 (s, 1H). ^{13}C NMR (101 MHz, DMSO) δ 152.43, 151.34–151.29 (d, J = 5.05), 149.87, 149.41, 143.41, 134.70, 130.90, 125.03, 122.27, 117.10, 113.22–113.30 (d, J = 8.1), 111.27–111.49 (d, J = 22.2), 97.15, 63.57, 48.12, 48.08. MS (EI) m/z 389.22 (M^++1). Anal. Calcd. for $C_{22}H_{21}FN_6$: C, 68.02; H, 5.45; N, 21.64. Found: C, 68.31; H, 5.20; N, 22.01.

*4-(4-(4-Chlorophenyl)piperazin-1-yl)-1-phenyl-1H-pyrazolo[3,4-d]pyrimidine (**13h**).* General Procedure **C**, yield 67%, white solid, mp 148–150 °C. ^{1}H NMR (400 MHz, DMSO-d_6) δ 3.31 (t, J = 8.31 Hz, 4H), 4.06 (t, J = 4.18 Hz, 4H), 7.90 (d, J = 8.32 Hz, 2H), 7.21–7.34 (m, 3H), 7.50–7.53 (m, 2H), 8.17 (d, J = 8.34 Hz, 2H), 8.37 (s, 1H), 8.51 (s, 1H). ^{13}C NMR (101 MHz, DMSO) δ 157.06, 155.72, 154.48, 149.62, 139.28, 135.23, 129.39, 129.14, 126.66, 123.01, 121.62, 116.98, 101.76, 47.79, 44.97. MS (EI) m/z 391.08 (M^++1). Anal. Calcd. for $C_{21}H_{19}ClN_6$: C, 64.53; H, 4.90; N, 21.50. Found: C, 64.17; H, 5.45; N, 22.01

*1-Phenyl-4-(4-(p-tolyl)piperazin-1-yl)-1H-pyrazolo[3,4-d]pyrimidine (**13i**).* General Procedure **C**, yield 67%, white solid, mp 152–154 °C. ^{1}H NMR (400 MHz, DMSO-d_6) δ 2.21 (s, 3H, C$\underline{H_3}$), 3.27 (t, J = 4.31 Hz, 4H), 4.11 (t, J = 4.22 Hz, 4H), 6.88 (d, J = 8.28 Hz, 2H), 7.06 (d, J = 8.05 Hz, 2H), 7.36 (t, J = 8.40 Hz, 1H), 7.55 (t, J = 7.95 Hz, 2H), 8.18 (d, J = 8.13, 2H), 8.40 (s, 1H), 8.60 (s, 1H). ^{13}C NMR (101 MHz, DMSO) δ 156.96, 155.85, 154.36, 148.93, 139.13, 135.48, 129.94, 129.54, 128.52, 126.81, 121.63, 116.28, 101.61, 48.86, 48.80, 20.50. MS (EI) m/z 371.16 (M^++1). Anal. Calcd. for $C_{22}H_{22}N_6$: C, 71.33; H, 5.99; N, 22.69. Found: C, 70.96; H, 6.03; N, 22.94.

*4-(4-(4-Nitrophenyl)piperazin-1-yl)-1-phenyl-1H-pyrazolo[3,4-d]pyrimidine (**13j**).* General Procedure **C**, yield 67%, yellow solid, mp 239–242 °C. ^{1}H NMR (400 MHz, DMSO-d_6) δ 3.76 (t, J = 4.38 Hz, 4H), 4.18 (t, J = 4.21 Hz, 4H), 6.94 (d, J = 8.30 Hz, 2H), 7.34 (t, J = 8.11 Hz, 1H), 7.53 (t, J = 7.98 Hz, 2H), 8.04–8.10 (m, 2H), 8.18 (d, J = 7.97 Hz, 2H), 8.40 (s, 1H), 8.48 (s, 1H). ^{13}C NMR (101 MHz, DMSO) δ 155.77, 154.38, 139.25, 137.46, 135.40, 129.44, 126.73, 126.14, 125.95, 121.60, 113.84, 112.23, 101.85, 45.47, 44.15. MS (EI) m/z 402.21 (M^++1). Anal. Calcd. for $C_{21}H_{19}N_7O_2$: C, 62.83; H, 4.77; N, 24.42. Found: C, 62.44; H, 4.94; N, 24.16.

*4-(4-(4-Methoxyphenyl)piperazin-1-yl)-1-phenyl-1H-pyrazolo[3,4-d]pyrimidine (**13k**).* General Procedure **C**, yield 67%, shiny white solid, mp 143–145 °C. ^{1}H NMR (400 MHz, DMSO-d_6) δ 3.15 (t, J = 4.41 Hz, 4H), 3.67 (s, 3H), 4.07 (t, J = 4.02 Hz, 4H), 6.80–6.92 (m, 4H), 7.33 (t, J = 7.89 Hz, 1H), 7.53 (t, J = 8.34 Hz, 2H), 8.18 (d, J = 8.43 Hz, 2H), 8.38 (s, 1H), 8.55 (s, 1H). ^{13}C NMR (101 MHz, DMSO) δ 156.89, 155.77, 154.34, 153.72, 145.37, 139.15, 135.36, 129.47, 126.71, 121.55, 118.22, 114.76, 101.59, 55.60, 49.95, 49.89. MS (EI) m/z 387.15 (M^++1). Anal. Calcd. for $C_{22}H_{22}N_6$:O: C, 68.38; H, 5.74; N, 21.75. Found C, 68.65; H, 6.07; N, 21.71.

*1-(1-Phenyl-1H-pyrazolo[3,4-d]pyrimidin-4-yl)piperidin-4-one (**13l**).* General Procedure **C**, yield 67%, white solid, mp 199–201 °C. ^{1}H NMR (400 MHz, DMSO-d_6) δ 2.62 (t, J = 6.20 Hz, 4H), 4.20 (t, J = 8.21 Hz, 4H), 7.33 (t, J = 7.46 Hz, 1H), 7.53 (t, J = 8.47 Hz, 2H), 8.17 (d, J = 7.99 Hz, 2H), 8.37 (s, 1H), 8.48 (s, 1H). ^{13}C NMR (101 MHz, DMSO) δ 207.93 (C=O), 156.78, 155.75, 154.19, 139.17, 135.58, 129.46, 126.66, 121.44, 101.83, 39.77, 39.71. MS (EI) m/z 393.20 (M^+). Anal. Calcd. for $C_{16}H_{15}N_5O$: C, 65.52; H, 5.15; N, 23.88. Found: C, 65.11; H, 5.42; N, 23.50.

*4-(4-(Methylsulfonyl)piperazin-1-yl)-1-phenyl-1H-pyrazolo[3,4-d]pyrimidine (**13m**).* A mixture of 4-chloro-1-phenyl-1*H*-pyrazolo[3,4-*d*]pyrimidine **12** (1 g, 4.34 mmol) and piperazine (1.1 g, 13 mmol) in 2–95% ethanol (30 mL) was refluxed for two hours. The reaction mixture was then concentrated and poured onto ice water (100 mL). The crude product was extracted with ethyl acetate (3 × 40 mL) and evaporated to give a white residue. Methyl sulfonyl chloride (0.4 mL, 3.6 mmol) was added slowly over 5 min to a 0 °C solution of the crude residue (1 g, 3.6 mmol) in CH_2Cl_2 (20 mL) containing few drops of triethylamine. The reaction mixture was stirred for 30 min at 0 °C then the ice bath was removed, and the reaction was stirred for 2 h at room temperature. The mixture was onto H_2O and the product was extracted with methylene chloride (3 × 40 mL). The organic layer was washed brine and dried over Na_2SO_4. The methylene chloride solution was concentrated and purified by flash column chromatography (SiO_2) using hexane/acetone (6:4) as eluent to give the methylsulfone derivative **13m** as a white solid (55%). mp 220–222 °C.

*4-(4,4-Difluoropiperidin-1-yl)-1-phenyl-1H-pyrazolo[3,4-d]pyrimidine (**14**).* Deoxofluor (1 mL, 5.5 mmol) was added slowly over 5 min to a 0 °C solution of *1-(1-phenyl-1H-pyrazolo[3,4-d]pyrimidin-4-yl)piperidin-4-one,* **13l** (2.16 g, 5.5 mmol) in CH_2Cl_2 (20 mL). The reaction mixture was stirred for 30 min at 0 °C then the ice bath was removed, and the reaction was stirred for 24 h at room temperature. The mixture was quenched with equivolume of H_2O and the product was extracted with methylene chloride (3 × 40 mL). The organic layer was washed with H_2O and brine and dried over Na_2SO_4. The methylene chloride solution containing the crude product was concentrated and purified by flash column chromatography (SiO_2) using hexane/ethyl acetate (8:2) as eluent to give the final compound **14** as a white solid (45%). mp 203–205 °C. ^{1}H NMR (400 MHz, DMSO-d_6) δ 2.10–2.18 (m, 2H), 2.38–2.43 (m, 2H), 4.06–4.18 (m, 4H), 7.34–7.39 (m, 1H), 7.53–7.57 (m, 2H), 8.15–8.17 (d, J = 8.19 Hz, 2H), 8.41 (s, 1H), 8.62 (s, 1H). MS (EI) m/z 316.26 (M^++1). Anal. Calcd. for $C_{16}H_{15}F_2N_5$: C, 60.94; H, 4.79; N, 22.21. Found: C, 61.13; H, 5.09; N, 22.17.

*1′-(1-Phenyl-1H-pyrazolo[3,4-d]pyrimidin-4-yl)spiro[chroman-2,4′-piperidin]-4-one (**15**).* Pyrrolidine (0.1 mL, 12 mmol) was added dropwise at room temperature to a solution of **13l** (1.82 g, 6 mmol) and 2-hydroxyacetophenone (0.85 g, 6 mmol) in anhydrous methanol (30 mL). The reaction mixture was refluxed overnight and then concentrated under reduced pressure. Ethyl acetate (50 mL) was added and the organic mixture was washed with 1 N HCl, then 1 N NaOH and brine. The organic layer was dried over Na_2SO_4, concentrated and purified by flash column chromatography (SiO_2) using hexane/ethyl acetate (8:2) as eluent to give the spiro derivative **15** as a white solid (79%). mp 178–180 °C. ^{1}H NMR (400 MHz, DMSO-d_6) δ 1.81 (t, J = 12.85 Hz, 2H), 2.06 (t, J = 18.86 Hz, 2H), 2.87 (s, 2H), 3.56 (t, J = 32.01 Hz, 2H), 4.49 (t, J = 24.26 Hz, 2H), 7.04–7.12 (m, 2H), 7.34 (t, J = 7.99 Hz, 1H), 7.51–7.61 (m, 3H), 7.76 (d, J = 8.19 Hz, 1H), 8.18 (d, J = 7.98 Hz, 2H), 8.36 (s, 1H), 8.53 (s, 1H). ^{13}C NMR (101 MHz, DMSO) δ

191.80 (C = O), 159.04, 156.68, 155.79, 154.37, 139.18, 136.93, 135.37, 129.47, 126.69, 126.34, 121.66, 121.54, 120.90, 118.88, 101.54, 78.55, 47.23, 33.56, 33.50. MS (EI) *m/z* 412.06 (M^++1). Anal. Calcd. for $C_{24}H_{21}N_5O_2$: C, 70.06; H, 5.14; N, 17.02. Found: C, 70.35; H, 5.11; N, 17.10.

*4-((1-(1-Phenyl-1H-pyrazolo[3,4-d]pyrimidin-4-yl)piperidin-4-yl) amino)benzenesulfonamide (**16**).* Sulfanilamide (1.0 g, 5.8 mmol) and 1-(1-phenyl-1*H*-pyrazolo[3,4-*d*]pyrimidin-4-yl)piperidin-4-one, **13l** (1.7 g, 5.8 mmol) were mixed in 1,2-dichloroethane (30 mL) and then treated with sodium triacetoxyborohydride (1.8 g, 8.12 mmol) and acetic acid (0.6 g, 10 mmol). The mixture was stirred at rt under a N_2 atmosphere for 24 h. The reaction mixture was quenched by adding 1 N NaOH, and the product was extracted with ethyl acetate. The organic extract was washed with brine and dried over $MgSO_4$. The solvent was evaporated and the residue was purified by flash column chromatography (SiO_2) using CH_2Cl_2/CH_3OH (9.5:0.5) as eluent to give the target compound **16** as a white solid (59%). mp 157–159 °C. ^{1}H NMR (400 MHz, DMSO-d_6) δ 3.22–3.37 (m, 5H), 3.89–3.98 (m, 4H), 4.42 (s, 1H, N<u>H</u>), 5.73 (br s, 2H, N<u>H</u>$_2$), 7.26–7.34 (m, 2H), 7.56 (t, *J* = 7.89 Hz, 1H), 7.73–7.83 (m, 3H), 7.98 (d, *J* = 8.11 Hz, 1H), 8.40 (d, *J* = 11.98 Hz, 2H), 8.58 (s, 1H), 8.75 (s, 1H). ^{13}C NMR (101 MHz, DMSO) δ 158.86, 155.62, 154.20, 139.00, 136.75, 135.20, 129.30, 126.51, 126.16, 121.36, 120.72, 118.70, 101.37, 57.36, 47.06, 33.38. MS (EI) *m/z* 449.33 (M^+). Anal. Calcd. for $C_{22}H_{23}N_7O_2S$: C, 58.78; H, 5.16; N, 21.81. Found: C, 59.01; H, 5.31; N, 22.16.

*1-(1-Phenyl-1H-pyrazolo[3,4-d]pyrimidin-4-yl)piperidin-4-ol (**17**).* To a solution of 1-(1-phenyl-1*H*-pyrazolo[3,4-*d*]pyrimidin-4-yl) piperidin-4-one, **13l** (1 g, 3.4 mmol) in MeOH (30 mL) was added $NaBH_4$ (0.25 g, 6.8 mmol) at 0 °C under argon. The reaction mixture was warmed to room temperature and left to stir for 2 h. The reaction mixture was quenched with water and extracted with ethyl acetate (3 × 30 mL). The organic extract was washed with saturated aqueous $NaHCO_3$ and brine and dried over Na_2SO_4. The solvent was concentrated and purified by flash column chromatography (SiO_2) using hexane/acetone (6:4) as eluent to give the compound **17** as a white solid (89%). mp 182–185 °C. ^{1}H NMR (400 MHz, DMSO-d_6) δ 1.140–1.52 (m, 2H), 1.78–1.89 (m, 1H), 3.28–3.64 (m, 4H), 3.83–3.87 (m, 1H), 4.29 (s, 1H, O<u>H</u>), 7.32–7.40 (m, 1H), 7.51–7.56 (m, 2H), 8.16 (d, *J* = 8.10 Hz, 2H), 8.18 (s, 1H), 8.55 (s, 1H). ^{13}C NMR (101 MHz, DMSO) δ 157.71, 152.28, 149.25, 138.67, 136.40, 129.61, 127.50, 122.13, 101.40, 65.66, 34.31, 34.25. MS (EI) *m/z* 296.26 (M^++1). Anal. Calcd. for $C_{16}H_{17}N_5O$: C, 65.07; H, 5.80; N, 23.71. Found: C, 65.34; H, 6.22; N, 23.53.

4.2. Pharmacology

4.2.1. Assay for cyclooxygenases (COXs) inhibition

Inhibition for Cox-1 and Cox-2 activity was determined by a colorimetric method using a Cox inhibitor screening assay kit (Cayman Chemical Ann Arbor, Michigan) in a total volume of 220 μL according to the directions provided with the kit manufacturer (Kulmacz and Lands, 1983). The inhibitory activities of the tested compounds were measured by monitoring the production of oxidized N, N, N′, N′-tetramethyl-p-phenylenediamine (TMPD) at 590 nm followed by incubation of either ovine COX-1 or COX-2 with arachidonic acid. The enzymes were preincubated for 5 min at 25 °C with the test compounds prior to addition of arachidonic acid (final concentration 1.1 mM) and TMPD and incubation for 5 min at 25 °C. Indomethacin was used as positive control. The COX-inhibiting activity was calculated according to the equation:

$$(\%\ \text{inhibition}) = [1 - (A_2 - A_0)/(A_1 - A_0)] \times 100$$

where A_0 is the absorbance of blank, A_1 was the absorbance of the vehicle control and A_2 is the absorbance in the presence of the test compound.

4.2.2. Assay for iNOS inhibition

The assay was performed using mouse macrophages (RAW264.7, obtained from ATCC). Cells were cultured in phenol red free RPMI medium supplemented with 10% bovine calf serum and 100 U/mL penicillin G sodium, and 100 μg/mL streptomycin at 37 °C in an atmosphere of 5% CO2 and 95% humidity as above. Cells were seeded in 96-well plates at 5 × 10^4 cells/well and incubated for 24 h. Test compounds diluted in serum free medium were added to the cells. After 30 min of incubation, LPS (5 μg/mL) was added and the cells were further incubated for 24 h. The concentration of nitric oxide (NO) was determined by measuring the level of nitrite released in the cell culture supernatant by using *Griess* reagent (Quang et al., 2006). Percent inhibition of nitrite production by the test compound was calculated in comparison to the vehicle control. IC_{50} values were obtained from dose curves. Parthenolide was used as positive control.

4.2.3. Assay for NF-κB inhibition

The assay was performed using human chondrosarcoma (SW1353, obtained from ATCC) cells as described earlier (Ma et al., 2007; Winter et al., 1962). Cells were cultured in 1:1 mixture of DMEM/F12 supplemented with 10% FBS, 100 U/mL penicillin G sodium, and 100 μg/mL streptomycin at 37 °C in an atmosphere of 5% CO_2 and 95% humidity. Cells (1.2 × 10^7) were washed once in an antibiotic and FBS-free DMEM/F12, and then re-suspended in 500 μL of antibiotic-free DMEM/F12 containing 2.5% FBS. NF-κB luciferase plasmid construct was added to the cell suspension at a concentration of 50 μg/mL and incubated for 5 min at room temperature. The cells were electroporated at 160 V and one 70-ms pulse using BTX disposable cuvettes model 640 (4-mm gap) in a BTX Electro Square Porator T 820 (BTX I, San Diego, CA). After electroporation, cells were plated to the wells of 96-well plates at a density of 1.25 × 10^5 cells per well. After 24 h, cells were treated with different concentrations of test compounds for 30 min prior to the addition of PMA (70 ng/mL) and incubated for 8 h. Luciferase activity was measured using the Luciferase Assay kit (Promega). The light output was detected on a SpectraMax plate reader. Percent inhibition of luciferase activity was calculated as compared to vehicle control and IC_{50} values were obtained from dose curves. Parthenolide was used as positive control. Sp-1 was used as a control transcription factor which is unresponsive to inflammatory mediators such as PMA. This is useful in detecting agents that nonspecifically inhibit luciferase expression due to cytotoxicity or inhibition of luciferase enzyme activity.

4.2.4. Assay for in vitro cytotoxicity assay

Cytotoxicity was determined against four human tumor cell lines [SK-MEL (malignant melanoma); KB (epidermal carcinoma, oral); BT-549 (ductal carcinoma, breast); SK-OV-3 (ovary carcinoma)] and two non-cancerous kidney cell lines [Vero cells (African green monkey kidney fibroblasts) and LLC-PK11 (pig kidney epithelial cells)] as described earlier in addition to Mouse leukemic monocyte macrophage cells (RAW 264.7) as described earlier (Mustafa et al., 2004). All the cell lines were obtained from ATCC and cultured in RPMI-1640 medium supplemented with bovine calf serum (10%) and amikacin (60 mg/L), at 37 °C, 95% humidity, 5% CO_2. Cells were seeded at a density of 25,000 cells/well and grown for 24 h. Test compounds, diluted in serum free medium, were added to the cells and incubated for 48 h. The number of viable cells was determined by Neutral Red assay (Borenfreund et al., 1990). Briefly, after treatment, cells were washed with saline and incubated for 3 h with the medium containing Neutral Red (166 μg/mL). The cells were washed to remove extracellular dye. A solution of acidified ethanol (0.33% HCl) was then added to lyse the cells; as a result, the incorporated dye was liberated from the viable cells. The absorbance was measured at 450 nm. IC_{50} was

Please cite this article in press as: Abdelazeem, A.H., et al. Novel pyrazolopyrimidine derivatives targeting COXs and iNOS enzymes; design, synthesis and biological evaluation as potential anti-inflammatory agents. Eur. J. Pharm. Sci. (2014), http://dx.doi.org/10.1016/j.ejps.2014.05.025

calculated from the dose curves generated by plotting percent growth vs. the test concentration on a logarithmic scale. Doxorubicin was used as positive control. All assays were performed in triplicate and the mean values are given in Table 1.

4.2.5. In vivo assays

Wistar rats (150–175 g) obtained from the National Research Center, Cairo, Egypt) were used throughout these studies and were kept at controlled conditions (temperature 23 ± 2 °C, humidity 60 ± 10%) and a 12/12 h light/dark cycle. All procedures relating to animal care and treatments were conducted in accordance with protocols approved by the Research Ethical Committee of Faculty of Pharmacy Beni-Suef University, Beni-Suef, Egypt (REC/BSU/P017B-2013).

4.2.5.1. Carrageenan-induced thermal hyperalgesia. Animals under light anesthesia received 100 μL of vehicle or carrageenan (1% in saline) s.c. on the plantar surface of the left hindpaw. The rats received orally vehicle, test compounds (10 mg/kg) or ketorolac (10 mg/kg) 2 h after carrageenan administration and were evaluated for paw hyperalgesia. Hyperalgesic responses to heat were measured at the indicated time points as described before (Hargreaves et al., 1988). A cutoff latency of 30 s was used to prevent heat-induced tissue damage. Rats were individually placed into plexiglass chambers. A high-intensity projector bulb (8-V, 50-watt) was used to deliver a focused thermal stimulus directly to individual hindpaws from beneath the chamber. The withdrawal latency period of paws was determined to the nearest 0.1 s. Each point represented the change (s) in withdrawal latency compared to vehicle-treated animals at each time point. Results are expressed as Paw-withdrawal latency change (s).

4.2.5.2. Carrageenan-induced rat paw edema assay. Rats were administered orally vehicle, test compounds (10 mg/kg) or ketorolac (10 mg/kg). Immediately thereafter, the rats received 100 μL of vehicle or carrageenan (1% in saline) s.c. on the plantar surface of the left hindpaw under light anesthesia, essentially, as reported before (Salvemini et al., 1996). The development of paw edema was assessed by measuring paw-volume changes at 1, 3 and 6 h after carrageenan injection using plethysmometer. The right hindpaw served as a reference of non-inflamed paw for comparison. Results are expressed as paw-volume change (mL).

4.2.5.3. Acetic acid-induced writhing assay. The writhing tests were carried as described before (Arrigoni-Martelli, 1979). Briefly, mice were administered orally vehicle, test compounds (10 mg/kg) or ketorolac (10 mg/kg) 30 minutes prior to intraperitoneal administration of 0.7% v/v acetic acid solution at 10 mL/kg body weight. The number of writhes (i.e., abdominal constriction followed by dorsiflexion and extension) occurring during a 20 min period beginning 5 min after acetic acid injection was measured. The results are expressed as the number of writhes per 20-min period.

4.3. Statistical analysis

Statistical analyses were performed by SPSS 9.0 software (SPSS Inc., Chicago, IL, USA). All results are presented as mean ± standard deviation (SD) values. Statistical differences between means were evaluated by one-way analysis of variance (ANOVA) followed by the Neuman–Keults test for multiple comparisons. Differences were considered significant at $P < 0.05$.

4.4. Docking study

Q4 The binding sites were generated from the co-crystallized ligands (IMM, SC-558 and AR-C120011) within COX-1, COX-2 and iNOS protein structures (PDB codes: 1PGF, 1CX2 and 3E65), respectively. Selected active pyrazolopyrimidine derivatives were energy minimized using CHARMm ForceField and then docked into the former prepared proteins active sites using LIGANDFIT imbedded into Discovery Studio Software with the following docking protocol: (i) number of Monte Carlo search trials = 30000, search step for torsions with polar hydrogens = 30°. (ii) The Root Mean Square Difference (RMS) threshold for ligand-to-binding site shape match was set to 2.0 employing a maximum of 1.0 binding site partitions and 1.0 site partition seed. (iii) The interaction energies were assessed employing Consistent Force Field (CFF) force field with a non-bonded cutoff distance of 10.0 Å and distance-dependent dielectric. An energy grid extending 3.0 Å from the binding site was implemented. (iv) Rigid body ligand minimization parameters were: 10 iterations of steepest descend (SD) minimization followed by 20 Broyden–Fletcher–Goldfarb–Shanno (BFGS) iterations applied to every successful orientation of the docked ligand. (v) A maximum of 10 diverse docked conformations/poses of optimal interaction energies were saved. (vi) The saved conformers/poses were further energy-minimized within the binding site for a maximum of 1000 rigid-body iterations.

Acknowledgments

We deeply thank Dr. Min Hye Yang and Ms. Katherine Martin for their excellent technical help and support in carrying out the *in vitro* bioassays.

References

Abdel-Magid, A.F., Carson, K.G., Harris, B.D., Maryanoff, C.A., Shah, R.D., 1996. Reductive amination of aldehydes and ketones with sodium triacetoxyborohydride. Studies on direct and indirect reductive amination procedures(1). J. Org. Chem. 61, 3849–3862.

Abunada, N.M., Hassaneen, H.M., Kandile, N.G., Miqdad, O.A., 2008. Synthesis and antimicrobial activity of some new pyrazole, fused pyrazolo[3,4-d]-pyrimidine and pyrazolo[4,3-e][1,2,4]-triazolo[1,5-c]pyrimidine derivatives. Molecules 13, 1501–1517.

Accelrys Software Inc., 2007. Discovery Studio Modeling Environment, Release 2.5. Accelrys Software Inc., San Diego.

Allison, M.C., Howatson, A.G., Torrance, C.J., Lee, F.D., Russell, R.I., 1992. Gastrointestinal damage associated with the use of nonsteroidal antiinflammatory drugs. N. Engl. J. Med. 327, 749–754.

Almansa, C., Alfon, J., de Arriba, A.F., Cavalcanti, F.L., Escamilla, I., Gomez, L.A., Miralles, A., Soliva, R., Bartroli, J., Carceller, E., Merlos, M., Garcia-Rafanell, J., 2003. Synthesis and structure–activity relationship of a new series of COX-2 selective inhibitors: 1,5-diarylimidazoles. J. Med. Chem. 46, 3463–3475.

Arrigoni-Martelli, E., 1979. Screening and assessment of antiinflammatory drugs. Methods Find. Exp. Clin. Pharmacol. 1, 157–177.

Bakavoli, M., Bagherzadeh, G., Vaseghifar, M., Shiri, A., Pordel, M., Mashreghi, M., Pordeli, P., Araghi, M., 2010. Molecular iodine promoted synthesis of new pyrazolo[3,4-*d*]pyrimidine derivatives as potential antibacterial agents. Eur. J. Med. Chem. 45, 647–650.

Bondock, S., Rabie, R., Etman, H.A., Fadda, A.A., 2008. Synthesis and antimicrobial activity of some new heterocycles incorporating antipyrine moiety. Eur. J. Med. Chem. 43, 2122–2129.

Borenfreund, E., Babich, H., Martin-Alguacil, N., 1990. Rapid chemosensitivity assay with human normal and tumor cells in vitro. In Vitro Cell. Dev. Biol. 26, 1030–1034.

Celano, M., Schenone, S., Cosco, D., Navarra, M., Puxeddu, E., Racanicchi, L., Brullo, C., Varano, E., Alcaro, S., Ferretti, E., Botta, G., Filetti, S., Fresta, M., Botta, M., Russo, D., 2008. Cytotoxic effects of a novel pyrazolopyrimidine derivative entrapped in liposomes in anaplastic thyroid cancer cells in vitro and in xenograft tumors in vivo. Endocr. Relat. Cancer 15, 499–510.

Chen, Y.L., 2000. Pyrazolopyrimidines for Treatment of CNS Disorders. United States Patent 6051578.

Cheng, C.C., Robins, R.K., 1956. Potential purine antagonists. VI. Synthesis of 1-Alkyl- and 1-Aryl-4-substituted pyrazolo[3,4-*d*]pyrimidines. J. Org. Chem. 21, 1240–1256.

Chern, J.H., Shia, K.S., Hsu, T.A., Tai, C.L., Lee, C.C., Lee, Y.C., Chang, C.S., Tseng, S.N., Shih, S.R., 2004. Design, synthesis, and structure–activity relationships of pyrazolo[3,4-*d*]pyrimidines: a novel class of potent enterovirus inhibitors. Bioorg. Med. Chem. Lett. 14, 2519–2525.

Cirino, G., Distrutti, E., Wallace, J.L., 2006. Nitric oxide and inflammation. Inflamm. Allergy Drug Targets 5, 115–119.

Clancy, R.M., Amin, A.R., Abramson, S.B., 1998. The role of nitric oxide in inflammation and immunity. Arthritis Rheum. 41, 1141–1151.

Cottam, H.B., Petrie, C.R., McKernan, P.A., Goebel, R.J., Dalley, N.K., Davidson, R.B., Robins, R.K., Revankar, G.R., 1984. Synthesis and biological activity of certain 3,4-disubstituted pyrazolo[3,4-*d*]pyrimidine nucleosides. J. Med. Chem. 27, 1119–1127.

Dannhardt, G., Kiefer, W., 2001. Cyclooxygenase inhibitors – current status and future prospects. Eur. J. Med. Chem. 36, 109–126.

Devesa, I., Alcaraz, M.J., Riguera, R., Ferrandiz, M.L., 2004. A new pyrazolo pyrimidine derivative inhibitor of cyclooxygenase-2 with anti-angiogenic activity. Eur. J. Pharmacol. 488, 225–230.

el-Bendary, E.R., Badria, F.A., 2000. Synthesis, DNA-binding, and antiviral activity of certain pyrazolo[3,4-*d*]pyrimidine derivatives. Arch. Pharm. (Weinheim) 333, 99–103.

Garcin, E.D., Arvai, A.S., Rosenfeld, R.J., Kroeger, M.D., Crane, B.R., Andersson, G., Andrews, G., Hamley, P.J., Mallinder, P.R., Nicholls, D.J., St-Gallay, S.A., Tinker, A.C., Gensmantel, N.P., Mete, A., Cheshire, D.R., Connolly, S., Stuehr, D.J., Aberg, A., Wallace, A.V., Tainer, J.A., Getzoff, E.D., 2008. Anchored plasticity opens doors for selective inhibitor design in nitric oxide synthase. Nat. Chem. Biol. 4, 700–707.

Ghosh, S., Karin, M., 2002. Missing pieces in the NF-kappaB puzzle. Cell 109 (Suppl.), S81–S96.

Gökhan, N., Erdogan, H., Tel, B., Demirdamar, R., 1996. Analgesic and antiinflammatory activity screening of 6-acyl-3-piperazinomethyl-2-benzoxazolinone derivatives. Eur. J. Med. Chem. 31, 625–628.

Guccionea, S., Modicaa, M., Longmoreb, J., Shawb, D., Barrettac, G., Santagatia, A., Santagatia, M., Russo, F., 1996. Synthesis and NK-2 antagonist effect of 1,6-diphenyl-pyrazolo[3,4-d]-thiazolo[3,2-a]4H-pyrimidin-4-one. Bioorg. Med. Chem. Lett. 6, 59–64.

Gund, P., Shen, T.Y., 1977. A model for the prostaglandin synthetase cyclooxygenation site and its inhibition by antiinflammatory arylacetic acids. J. Med. Chem. 20, 1146–1152.

Hargreaves, K., Dubner, R., Brown, F., Flores, C., Joris, J., 1988. A new and sensitive method for measuring thermal nociception in cutaneous hyperalgesia. Pain 32, 77–88.

Ialenti, A., Ianaro, A., Moncada, S., Di Rosa, M., 1992. Modulation of acute inflammation by endogenous nitric oxide. Eur. J. Pharmacol. 211, 177–182.

Ianaro, A., O'Donnell, C.A., Di Rosa, M., Liew, F.Y., 1994. A nitric oxide synthase inhibitor reduces inflammation, down-regulates inflammatory cytokines and enhances interleukin-10 production in carrageenin-induced oedema in mice. Immunology 82, 370–375.

Kulmacz, R.J., Lands, W.E., 1983. Requirements for hydroperoxide by the cyclooxygenase and peroxidase activities of prostaglandin H synthase. Prostaglandins 25, 531–540.

Kurumbail, R.G., Stevens, A.M., Gierse, J.K., McDonald, J.J., Stegeman, R.A., Pak, J.Y., Gildehaus, D., Miyashiro, J.M., Penning, T.D., Seibert, K., Isakson, P.C., Stallings, W.C., 1996. Structural basis for selective inhibition of cyclooxygenase-2 by anti-inflammatory agents. Nature 384, 644–648.

Lim, K.M., Lee, J.Y., Lee, S.M., Bae, O.N., Noh, J.Y., Kim, E.J., Chung, S.M., Chung, J.H., 2009. Potent anti-inflammatory effects of two quinolinedione compounds, OQ1 and OQ21, mediated by dual inhibition of inducible NO synthase and cyclooxygenase-2. Br. J. Pharmacol. 156, 328–337.

Looker, D.L., Marr, J.J., Berens, R.L., 1986. Mechanisms of action of pyrazolopyrimidines in Leishmania donovani. J. Biol. Chem. 261, 9412–9415.

Ma, G., Khan, S.I., Benavides, G., Schuhly, W., Fischer, N.H., Khan, I.A., Pasco, D.S., 2007. Inhibition of NF-kappaB-mediated transcription and induction of apoptosis by melampolides and repandolides. Cancer Chemother. Pharmacol. 60, 35–43.

Ma, L., Xie, C., Ma, Y., Liu, J., Xiang, M., Ye, X., Zheng, H., Chen, Z., Xu, Q., Chen, T., Chen, J., Yang, J., Qiu, N., Wang, G., Liang, X., Peng, A., Yang, S., Wei, Y., Chen, L., 2011. Synthesis and biological evaluation of novel 5-benzylidenethiazolidine-2,4-dione derivatives for the treatment of inflammatory diseases. J. Med. Chem. 54, 2060–2068.

MacMicking, J., Xie, Q.W., Nathan, C., 1997. Nitric oxide and macrophage function. Annu. Rev. Immunol. 15, 323–350.

Mesangeau, C., Narayanan, S., Green, A.M., Shaikh, J., Kaushal, N., Viard, E., Xu, Y.T., Fishback, J.A., Poupaert, J.H., Matsumoto, R.R., McCurdy, C.R., 2008. Conversion of a highly selective sigma-1 receptor-ligand to sigma-2 receptor preferring ligands with anticocaine activity. J. Med. Chem. 51, 1482–1486.

Micklewright, R., Lane, S., Linley, W., McQuade, C., Thompson, F., Maskrey, N., 2003. Review article: NSAIDs, gastroprotection and cyclo-oxygenase-II-selective inhibitors. Aliment. Pharmacol. Ther. 17, 321–332.

Mustafa, J., Khan, S.I., Ma, G., Walker, L.A., Khan, I.A., 2004. Synthesis and anticancer activities of fatty acid analogs of podophyllotoxin. Lipids 39, 167–172.

Natarajan, S.K., Moreno, O., Graddis, T.J., Duncan, D., Laus, R., Chen, F., 2005. Compositions and methods using small mol. Trp-p8 Modulators for the Treatment of Diseases Associated with Trp-p8 Expression. Patent WO 2005020897.

Peri, K.G., Hardy, P., Li, D.Y., Varma, D.R., Chemtob, S., 1995. Prostaglandin G/H synthase-2 is a major contributor of brain prostaglandins in the newborn. J. Biol. Chem. 270, 24615–24620.

Quang, D.N., Harinantenaina, L., Nishizawa, T., Hashimoto, T., Kohchi, C., Soma, G., Asakawa, Y., 2006. Inhibition of nitric oxide production in RAW 264.7 cells by azaphilones from xylariaceous fungi. Biol. Pharm. Bull. 29, 34–37.

Quintela, J.M., Peinador, C., Gonzalez, L., Devesa, I., Ferrandiz, M.L., Alcaraz, M.J., Riguera, R., 2003. 6-Dimethylamino 1H-pyrazolo[3,4-*d*]pyrimidine derivatives as new inhibitors of inflammatory mediators in intact cells. Bioorg. Med. Chem. 11, 863–868.

Raffa, D., Maggio, B., Plescia, F., Cascioferro, S., Raimondi, M.V., Plescia, S., Cusimano, M.G., 2009. Pyrazolo[3,4-*d*]pyrimidine derivatives as COX-2 selective inhibitors: synthesis and molecular modelling studies. Arch. Pharm. (Weinheim) 342, 321–326.

Rathod, I.S., Baheti, K.G., Shirsath, V.S., 2005. Synthesis and analgesic activity of 2-(un) substituted-3-amino-5-aryl-6-phenyl pyrazolo(3,4-d)pyrimidine-4-(5H)-ones. Ind. J. Pharm. Sci. 67, 593–597.

Robichaud, J., Black, W.C., Therien, M., Paquet, J., Oballa, R.M., Bayly, C.I., McKay, D.J., Wang, Q., Isabel, E., Leger, S., Mellon, C., Kimmel, D.B., Wesolowski, G., Percival, M.D., Masse, F., Desmarais, S., Falgueyret, J.P., Crane, S.N., 2008. Identification of a nonbasic, nitrile-containing cathepsin K inhibitor (MK-1256) that is efficacious in a monkey model of osteoporosis. J. Med. Chem. 51, 6410–6420.

Salgin-Goksen, U., Gokhan-Kelekci, N., Goktas, O., Koysal, Y., Kilic, E., Isik, S., Aktay, G., Ozalp, M., 2007. 1-Acylthiosemicarbazides, 1,2,4-triazole-5(4H)-thiones, 1,3,4-thiadiazoles and hydrazones containing 5-methyl-2-benzoxazolinones: synthesis, analgesic-anti-inflammatory and antimicrobial activities. Bioorg. Med. Chem. 15, 5738–5751.

Salvemini, D., Manning, P.T., Zweifel, B.S., Seibert, K., Connor, J., Currie, M.G., Needleman, P., Masferrer, J.L., 1995. Dual inhibition of nitric oxide and prostaglandin production contributes to the antiinflammatory properties of nitric oxide synthase inhibitors. J. Clin. Invest. 96, 301–308.

Salvemini, D., Wang, Z.Q., Wyatt, P.S., Bourdon, D.M., Marino, M.H., Manning, P.T., Currie, M.G., 1996. Nitric oxide: a key mediator in the early and late phase of carrageenan-induced rat paw inflammation. Br. J. Pharmacol. 118, 829–838.

Seibert, K., Zhang, Y., Leahy, K., Hauser, S., Masferrer, J., Perkins, W., Lee, L., Isakson, P., 1994. Pharmacological and biochemical demonstration of the role of cyclooxygenase 2 in inflammation and pain. Proc. Natl. Acad. Sci. USA 91, 12013–12017.

Seminerio, M.J., Robson, M.J., Abdelazeem, A.H., Mesangeau, C., Jamalapuram, S., Avery, B.A., McCurdy, C.R., Matsumoto, R.R., 2012. Synthesis and pharmacological characterization of a novel sigma receptor ligand with improved metabolic stability and antagonistic effects against methamphetamine. AAPS J. 14, 43–51.

Spreafico, A., Schenone, S., Serchi, T., Orlandini, M., Angelucci, A., Magrini, D., Bernardini, G., Collodel, G., Di Stefano, A., Tintori, C., Bologna, M., Manetti, F., Botta, M., Santucci, A., 2008. Antiproliferative and proapoptotic activities of new pyrazolo[3,4-*d*]pyrimidine derivative Src kinase inhibitors in human osteosarcoma cells. FASEB J. 22, 1560–1571.

Trivedi, A., Vaghasiya, S., Dholariya, B., Dodiya, D., Shah, V., 2010. Synthesis and antimycobacterial evaluation of various 6-substituted pyrazolo[3,4-*d*]pyrimidine derivatives. J. Enzyme Inhib. Med. Chem. 25, 893–899.

Trivedi, A.R., Dholariya, B.H., Vakhariya, C.P., Dodiya, D.K., Ram, H.K., Kataria, V.B., Siddiqui, A.B., Shah, V.H, 2012. Synthesis and anti-tubercular evaluation of some novel pyrazolo[3,4-*d*]pyrimidine derivatives. Med. Chem. Res. 8, 1887–1891.

Viaud, M.C., Jamoneau, P., Flouzat, C., Bizot-Espiard, J.G., Pfeiffer, B., Renard, P., Caignard, D.H., Adam, G., Guillaumet, G., 1995. N-substituted oxazolo[5,4-b]pyridin-2(1H)-ones: a new class of non-opiate antinociceptive agents. J. Med. Chem. 38, 1278–1286.

Winter, C.A., Risley, E.A., Nuss, G.W., 1962. Carrageenin-induced edema in hind paw of the rat as an assay for antiiflammatory drugs. Proc. Soc. Exp. Biol. Med. 111, 544–547.

Wolfe, M.M., Lichtenstein, D.R., Singh, G., 1999. Gastrointestinal toxicity of nonsteroidal antiinflammatory drugs. N. Engl. J. Med. 340, 1888–1899.

Xia, Y., Chackalamannil, S., Czarniecki, M., Tsai, H., Vaccaro, H., Cleven, R., Cook, J., Fawzi, A., Watkins, R., Zhang, H., 1997. Synthesis and evaluation of polycyclic pyrazolo[3,4-*d*]pyrimidines as PDE1 and PDE5 cGMP phosphodiesterase inhibitors. J. Med. Chem. 40, 4372–4377.

Yewale, S.B., Ganorkar, S.B., Baheti, K.G., Shelke, R.U., 2012. Novel 3-substituted-1-aryl-5-phenyl-6-anilinopyrazolo[3,4-d]pyrimidin-4-ones: docking, synthesis and pharmacological evaluation as a potential anti-inflammatory agents. Bioorg. Med. Chem. Lett. 22, 6616–6620.

Yoshimura, H., Sekine, S., Adachi, H., Uematsu, Y., Mitani, A., Futaki, N., Shimizu, N., 2011. High levels of human recombinant cyclooxygenase-1 expression in mammalian cells using a novel gene amplification method. Protein Expr. Purif. 80, 41–46.

Please cite this article in press as: Abdelazeem, A.H., et al. Novel pyrazolopyrimidine derivatives targeting COXs and iNOS enzymes; design, synthesis and biological evaluation as potential anti-inflammatory agents. Eur. J. Pharm. Sci. (2014), http://dx.doi.org/10.1016/j.ejps.2014.05.025